Available online at www.sciencedirect.com
SCIENCE DIRECT®
Journal of Chromatography A, 1090 (2005) 16–38
JOURNAL OF CHROMATOGRAPHY A
www.elsevier.com/locate/chroma

Effects of high pressure in liquid chromatography

Michel Martin[a], Georges Guiochon[b,c,*]

[a] *Laboratoire de Physique et Mécanique des Milieux Hétérogènes, École Supérieure de Physique et de Chimie Industrielles, 10 Rue Vauquelin, F-75231 Paris Cedex 05, France*
[b] *Department of Chemistry, University of Tennessee, 552 Buehler Hall, Knoxville, TN 37996 1600, USA*
[c] *Division of Chemical Sciences, Oak Ridge National Laboratory, Oak Ridge, TN 37831 6120, USA*

Received 3 May 2005; accepted 1 June 2005
Available online 3 August 2005

Abstract

All the experimental parameters that the chromatographers are used to consider as constant (the column length and its diameter, the particle size, the column porosities, the phase ratio, the column hold-up volume, the pressure gradient along the column, the mobile phase density and its viscosity, the diffusion coefficients, the equilibrium constants, the retention factors, the efficiency parameters) depend on pressure to some extent. While this dependence is negligible as long as experiments, measurements, and separations are carried out under conventional pressures not exceeding a few tens of megapascal, it is no longer so when the inlet pressure becomes much larger and exceeds 100 MPa. Equations are developed to determine the extent of the influence of pressure on all these parameters and to account for it. The results obtained are illustrated with graphics. The essential results are that (1) many parameters depend on the inlet pressure, hence on the flow rate; (2) the apparent reproducibility of parameters as simple as the retention factor will be poor if measurements are carried out at different flow rates, unless due corrections are applied to the results; (3) the influence of the temperature on the equilibrium constants should be studied under constant inlet pressure rather than at a constant flow rate, to minimize the coupling effect of pressure and temperature through the temperature dependence of the viscosity; and (4) while reproducibility of results obtained at constant pressure and flow rate will not be affected, method development becomes far more complex because of the pressure dependence of everything.

Keyword: Pressure

1. Introduction

The recent advent of combinatorial chemistry has increased considerably the number of analyses that must be performed in the analytical services of companies involved in the synthesis and development of fine chemicals, particularly in the pharmaceutical industry. This has brought back to the forefront of the preoccupation of chromatographers the perennial optimization problem of analytical chromatography. The experimental conditions under which the analyses are carried out must be adjusted in order to minimize their duration while achieving the separations needed and keeping the detection sensitivity as high as possible. Several waves of progress have taken place in the past, each one ending with the commercial availability of shorter columns, packed with smaller particles, operated under higher pressures, and generating faster analyses than the columns of the previous generation. The most recent of these waves occurred over 20 years ago and lead to the development of the now conventional 10–20 cm long columns, packed with 3–5 μm particles, and operated at flow rates of a few mL/min (for a column i.d. of about 4 mm), under inlet pressures of 40– 50 MPa (1 MPa = 10 bar). There is now a strong demand for improved performance. Several approaches have been suggested and are currently pursued actively. The most straightforward of them is the preparation of conventional columns packed with very fine particles, in the 1– 2 μm range, and operated at higher flow rates than columns packed with the now classical 3–5 μm particles. This requires extremely high inlet pressures,

* Corresponding author. Tel.: +1 865 974 0733; fax: +1 865 974 2667.
E-mail address: guiochon@utk.edu (G. Guiochon).

0021-9673/$ – see front matter © 2005 Elsevier B.V. All rights reserved.
doi:10.1016/j.chroma.2005.06.005

in the low kbar range. The operation of HPLC columns under such high inlet pressures is now seriously considered [1].

The most important alternative approaches are the development of fast monolithic columns and that of open tubular columns. Monolithic columns are a recent acquisition of HPLC [2–4]. They exhibit a permeability that is an order of magnitude higher than that of packed columns while having comparable performance. They can generate higher efficiencies under higher mobile phase flow velocities than packed columns while being operated at a lower pressure. It is likely that some modifications of their current method of preparation could allow the production of still faster and more efficient columns, at the possible cost of a higher inlet pressure that could be accommodated by classical equipments. After all, these columns have been manufactured and used for barely 5 years. In principle, microbore open tubular columns could afford considerable improvements over current performance by allowing analysis times of the order of seconds with efficiencies at least as high as those that are currently achieved with the best packed columns [5]. However, the enormous technical difficulties that must be overcome [6] have prevented the development of commercial instruments based on their use. Detection sensitivity will remain a major obstacle because these columns can accept only extremely small samples.

No fundamental difficulties should be expected in the preparation and use of more efficient, faster columns that would be packed with particles finer than those currently available. It is obvious that most chromatographers consider pressure and its effects with benign contempt. The initial reluctance of biochemists that was referred to as *barophobia* by Csaba Horváth was not justified and has faded away. Under pressures lower than several kbar, protein molecules remain as stable as under atmospheric pressure [7,8]. Yet, certain pressure effects can be treacherous under certain conditions. About 30 years ago, instrument manufacturers who attempted to manufacture syringe pumps for liquid chromatography failed because it was too difficult at the time to control properly the pressure excursion in the cylinder while delivering a constant flow rate of the mobile phase [9–11].

Pressure affects significantly the specific volume, the viscosity, the freezing points of liquids and other phase changes or transitions. It also affects diffusion coefficients (that tends to be inversely proportional to the mobile phase viscosity) and equilibrium constants. The unavoidable consequences of these effects are that many chromatographic results become pressure sensitive, which means that they change with the column flow rate since it is impossible to adjust the flow velocity along a column without changing the inlet pressure, hence the pressure gradient along this column. We review here the physico-chemical background of chromatography under high pressures, up to the low kilobar range.

In the first part of this review, we review under the heading *"Theory"* the influence of the pressure on each of the isolated parameters that are successively studied and discussed. The integrated or combined influences of all the parameters involved in the chromatographic process (the pressure, the mobile phase flow rate, its compressibility and its viscosity, the retention factor, the column porosities, permeability and dimensions) on the peak retention time, the elution peak profile, and the profiles of flow and pressure along the column are discussed in a second part, under the heading *"Results and discussion"*.

2. Theory

2.1. Influence of the pressure on the melting point of a solvent

This effect is surprisingly important and may have nefarious consequences because they are rarely, if ever, anticipated. Years ago, we tried and used cyclohexane as the mobile phase for some separations. Unexpectedly, the alumina piston of the HPLC pump broke when we needed to operate it at ca. 200 bar. We eventually found that this breakage was caused by cyclohexane solidifying when compressed in the pump under this pressure, immobilizing the piston [12]. Such incidents might become more likely if high pressure operations become popular.

For any phase change, the variation of the temperature, T_f, of a phase change is related to that of the pressure, P, by means of the Clapeyron equation

$$\frac{dT_f}{dP} = \frac{\Delta V_t}{\Delta S_t} \quad (1)$$

where ΔS_t is the entropy change and ΔV_t is the volume change associated with the phase transition considered. Alternatively, Eq. (1) can written

$$\frac{dT_f}{dP} = \frac{T\Delta V_t}{\Delta H_t} \quad (2)$$

where ΔH_t is the latent heat of the phase change. For fusion (i.e., the solid–liquid transform), the entropy of a liquid being always larger than that of the solid, ΔH_t is positive. For most substances, the specific volume of the liquid is larger than that of the solid and ΔV_t is also positive. Consequently, for most substances, the temperature of fusion increases with increasing pressure. Water is a rare but most noticeable exception (together with a few elements and salts, e.g., bismuth, gallium, silicium, copper chloride) because the density of liquid water is larger than that of ice. The latent heat of fusion of water is 333.5 J g^{-1}, and the densities of liquid water and ice at atmospheric pressure at 273.15 K are 0.9998 and 0.917 g cm^{-3}, respectively [13]. If we assume that ΔH_t and the densities are practically constant over the pressure range of interest, we obtain $dT/dP = -7.4 \times 10^{-3}$ K bar^{-1}. Hence, water melts at −7.4 K under a pressure of 1000 bar. For all solvents used in chromatography, however, the melting point increases with increasing pressure.

The empirical Simon equation [14] relates the pressure, P_f, and the temperature, T_f, of fusion of a compound as

$$P_f = P_t + a_1 \left[\left(\frac{T_f}{T_t} \right)^{c_1} - 1 \right] \quad (3)$$

where P_t and T_t (K) are the pressure and the temperature of the triple point of the compound studied, a_1 and c_1 are two empirical parameters which are tabulated for various substances [15]. P_t is usually very small (of the order of 1 mbar) and can be neglected. T_t is very close to the normal melting point under atmospheric pressure (and, correlatively, a_1 is usually much larger than 1 bar). Values of the melting pressures at 20 and 30 °C were calculated using Eq. (3) for some substances for which these pressures are below 10 kbar (1 GPa). The results are reported in Table 1. From this table, it is clear that the lower the melting point under atmospheric pressure, the higher the melting pressure at 20 or 30 °C. Almost all the solvents used in reversed phase and in normal phase HPLC have melting points below 0 °C under atmospheric pressure (note that the value calculated for cyclohexane agrees well with the one that we found) and no serious difficulties should be expected up to pressures of a few kilobar (unless separations at subambient temperatures are considered).

Fig. 1 shows the variations of the temperature of fusion with the local pressure for some solvents commonly used as main components of the mobile phase in HPLC, computed according to Eq. (3), using data of ref. [15], except for methanol, for which the reported value of dP_f/dT has been assumed to remain constant in the whole pressure range considered here.

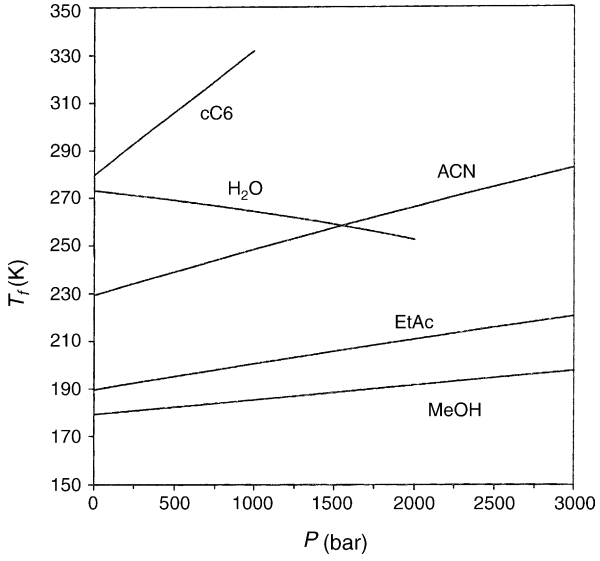

Fig. 1. Plot of the temperature of fusion, T_f, of various compounds vs. the local pressure, P. *Symbols*: cC6, cyclohexane; H_2O, water; ACN, acetonitrile; EtAc, ethyl acetate; MeOH, methanol. The curves are limited to the pressure domain within which the determination of the two empirical parameters of Eq. (3), a_1 and c_1 has been made.

2.2. Influence of the pressure on the specific volumes of liquids

2.2.1. Pressure and specific volume

The behavior of liquids under the pressures that can reasonably be achieved and safely handled in the laboratory, i.e., up to a few kbar, has been the topic of intensive studies and much pertinent data is available [16–18]. Table 2 summarizes the compressibility of a number of common solvents.

As a first approximation, the compressibility of liquids can be considered as constant at constant temperature in the range of pressures used in conventional HPLC (below 40 MPa or so), at least as far as the column flow rate and the pressure gradient along the column are concerned. However, in the range of pressures considered here, the compressibility does depend on the pressure. Up to several kbar, the pressure dependence of the volume, $V_{p,T}$, occupied by a given mass of

Table 1
Melting pressure of some solvents

	P_f[b] (20 °C)	P_f[b] (30 °C)	T_f (°C, at $P = 1$ bar)
Acetonitrile (CH_3CN)	3656	4315	−45.7
Aniline ($C_6H_5NH_2$)	1319	1863	−6.3
Bromobenzene (C_6H_5Br)	2885	3546	−30.8
Bromoform ($CHBr_3$)	487	901	8.3
Carbon tetrachloride (CCl_4)	1151	1451	−23.0
Chloroform ($CHCl_3$)	5531	6256	−63.5
4-Chlorotoluene (C_7H_7Cl)	451	844	7.5
Cyclohexane (C_6H_{12})	251	441	6.5
1,4-Dioxane ($C_4H_8O_2$)	758	1702	11.8
Dodecane ($C_{12}H_{26}$)	1353	1881	−9.6
Ethylene chloride ($C_2H_4Cl_2$)	2915	3502	−35.4
Nitrobenzene ($C_6H_5NO_2$)	527	904	5.7
o-Xylene[a] (C_7H_{10})	1921	2346	−25.2
p-Xylene (C_7H_{10})	191	485	13.3

[a] Values calculated from experimental data reported for dP_f/dT [15].
[b] P_f in bar.

Table 2
Compressibility of some common solvents

	Temperature (°C)	Compressibility[a] (χ) ($\times 10^4$)	c (Eq. (4))	b[b] (Eq. (4))
n-Pentane	25	3.14	0.0943	299.6
n-Hexane	25	1.61	0.0943	587
n-Heptane	0	1.18	0.0943	799
n-Heptane	25	1.42	0.0943	662
n-Heptane	40	1.60	0.0943	591
n-Heptane	60	1.87	0.0943	505
n-Octane	25	1.20	0.0943	787
Benzene	25	0.96	0.0938	970
Methylene chloride	25	0.97	0.1038	1066
Chloroform	25	0.97	0.1038	1066
Carbon tetrachloride	25	1.07	0.0925	867
Diethyl ether	20	1.87	0.235	1260
Acetone	25	1.24	0.1023	826
Methanol	20	1.23	0.148	1210
Ethanol	20	1.11	0.209	1890
Water	25	0.46	0.1368	2996
Acetonitrile	25	1.10	0.128	1162

[a] χ in bar^{-1}.
[b] b in bar.

liquid at temperature T is well accounted for by Tait equation [19]

$$\frac{V_{p,T} - V_{p_0,T}}{V_{p_0,T}} = c \ln \frac{P_0 + b}{P + b} \quad (4)$$

or

$$\left(\frac{P_0 + b}{P + b}\right)^c = e^{((V/V_0)-1)} \quad (5)$$

V_0 being the specific volume, $V_{p_0,T}$, under the reference pressure P_0. For the liquids considered here, c is small and it is independent of the pressure (Table 2). The variations of V/V_0 versus P for various common liquids, according to Eq. (5), are shown in Fig. 2. Because the variation of the specific volume with pressure is small or moderate, V/V_0 is not very different from unity and Eq. (4) may be expended as a Taylor series:

$$\left(\frac{P_0 + b}{P + b}\right)^c = \frac{V}{V_0} + \frac{1}{2}\left(\frac{V}{V_0} - 1\right)^2 + \frac{1}{6}\left(\frac{V}{V_0} - 1\right)^3 + \cdots \quad (6)$$

At pressures below 0.5 kbar, Eq. (5) can be limited to the first term of the expansion without significant loss of accuracy and we have

$$\left(\frac{P_0 + b}{P + b}\right)^c = \frac{V}{V_0} \quad (7)$$

At higher pressures the use of a two-term expansion provides a more accurate relationship.

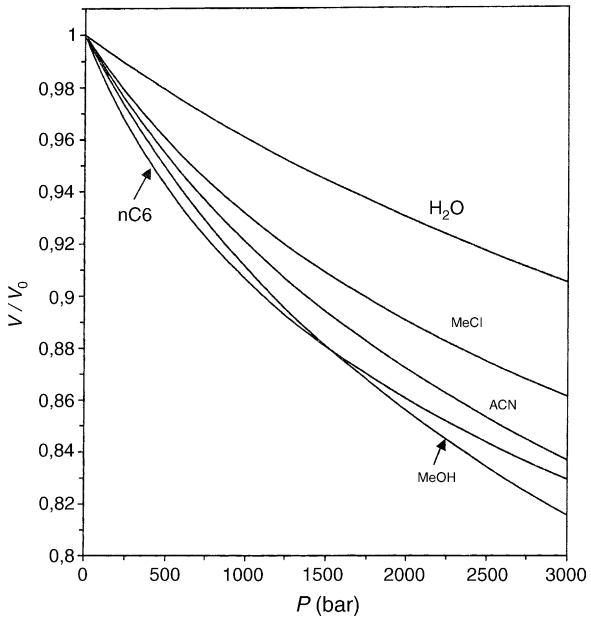

Fig. 2. Ratio of the specific volume, V, of several solvents to their specific volume under the atmospheric pressure, V_0, vs. the pressure, P, at 25 °C. *Symbols*: *n*C6, *n*-hexane; H_2O, water; MeCl, methylene chloride; ACN, acetonitrile; MeOH, methanol.

2.2.2. Compressibility

The compressibility of a material is defined as

$$\chi = -\frac{1}{V}\frac{dV}{dP} \quad (8)$$

The compressibility is always positive. It varies with the pressure. Differentiation of Eq. (6) and combination with Eq. (7) gives

$$\chi = \frac{c}{P + b} \quad (9)$$

The compressibility of liquids decreases slowly with increasing pressure. Eq. (8) shows that the compressibility decreases by half when the pressure increases from 0 to b [bar]. From the data in Table 2 and Eq. (8), we see that for most liquids, b is between 0.8 and 3 kbar.

Note that both b and c depend on the temperature. Correlations are available in the literature. As long as the temperature is not important compared to the critical temperature, so the reduced temperature is low, the temperature and the pressure dependence of the specific volume of the mobile phase can be considered independently. Closer to the critical state, the situation would complicate considerably. This issue is outside the scope of this review.

2.3. Influence of pressure on the viscosity of liquids

The viscosity of liquids increases with increasing pressure. Water below ca. 20 °C is a rare exception. In the pressure range up to a few kbar, this variation is nearly linear:

$$\eta = \eta_0[1 + \alpha(P - P_0)] \quad (10)$$

where η_0 is the velocity under the reference pressure (P_0) and α is the relative variation of the viscosity per unit pressure. Values of η_0 and α, when the atmospheric pressure is taken as the reference pressure, are reported from Smithsonian Physical Tables in Table 3 for a variety of solvents. In this table, α is given as $(\eta_{1000} - \eta_0)/(999\eta_0)$, where η_{1000} is the viscosity at 1 kbar, which linearizes the pressure–viscosity relationship. The actual difference between the true and the calculated value of η may be of the order of 5% in the pressure range up to 1 kbar. Under higher pressures, it might be higher. The ratio of the actual viscosity, η, to the viscosity under atmospheric pressure, η_0, is plotted versus the pressure in Fig. 3, according to Eq. (10) and to some of the data in Table 3.

A correlation due to Lucas [20] shows that Eq. (10) is valid as long as the reduced temperature is not very large, which is the case for all the mobile phases used in HPLC (at least as long as HPLC is not carried out at high temperatures). It would not apply to carbon dioxide in a straightforward manner but, then, a more complex correlation would allow a rather accurate prediction of the dependence of the viscosity on the temperature and the pressure in the column [21]. A recent publication reports that the apparent viscosity of a 50:50 mixture of water and acetonitrile in-

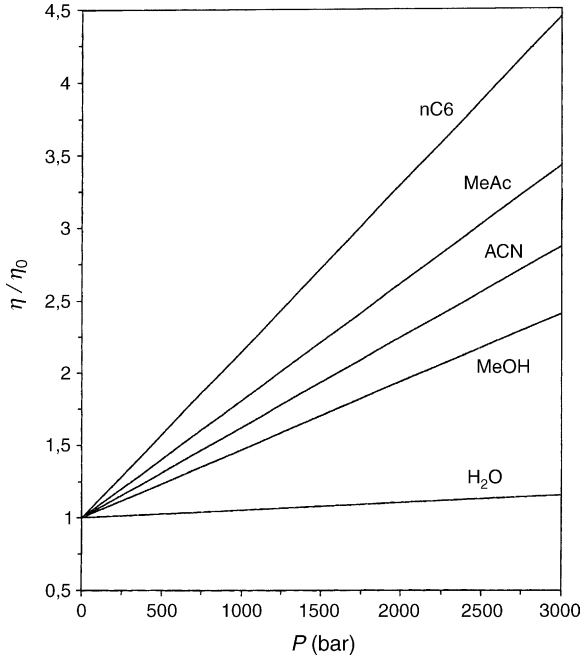

Fig. 3. Ratio of the viscosity under pression P, η, to the viscosity under atmospheric pressure, η_0, vs. the pressure, P, for various liquids at 30 °C. *Symbols*: *n*C6, *n*-hexane; MeAc, methyl acetate; ACN, acetonitrile; MeOH, methanol; H_2O, water.

creases by 34% when the inlet pressure of a column percolated by this solution is raised from 140 to 4800 bar [22]. This number seems consistent with others reported here, although there are no numerical data for almost any mixtures of solvents in the literature. We must note, however, that the effect of pressure on the viscosity is linear and that, if the pressure drop is 4800 bar, the increase measured corresponds to an increase of the average pressure of only 2400 bar. The actual increase of the viscosity of the solution is thus of 68% when the pressure is increased from 1 to 4800 bar.

2.4. Influence of the pressure on the diffusion coefficients in liquids

As a first approximation, we can assume with Wilke and Chang [23] that the product, $D^0_{AB}\eta_B$, of the diffusion coefficient of a dilute species, A, in a solvent B and the viscosity of this solvent is constant. This is in agreement with the results of Tyn and Calus [24]. There are few detailed investigations on this issue. Easteal [25] showed that the self-diffusion coefficient of *n*-hexane decreases from 4.2×10^{-5} cm^2 s^{-1} to 0.7×10^{-5} cm^2 s^{-1} when the pressure increases from 1 to 3500 bar. This six-fold decrease could have serious consequences regarding the column efficiency. Easteal [25] also suggested the following correlation to account for his data

$$\ln D_i^* = a_2 + \xi P^m \tag{11}$$

where D_i^* is the tracer or self-diffusion coefficient of compound i, a_2 and ξ are numerical constants that vary slowly with the temperature, and m is a numerical coefficient close to 0.75. The coefficient ξ is negative and diffusion coefficients decrease with increasing pressure. Eq. (11) can be used to estimate high-pressure diffusion coefficients. The ratio of the self-diffusion coefficient, D^*, under the pressure P to the self-diffusion coefficient under the atmospheric pressure, D_0^*, is plotted versus P in Fig. 4 for various liquids, according to Eq. (11) and using the values of the parameters ξ and m that are reported in [26]. The curve for water does not follow Eq. (11). It was drawn using experimental data [27].

Both viscosity and diffusion are activation processes. While the viscosity decreases with increasing temperature, the diffusion coefficient increases and, in agreement with the practical constancy of the product $D^0_{AB}\eta_B$, the absolute values of the two activation energies are close. They certainly have the same order of magnitude. This relationship remains valid under pressure. As pointed out [28], the relative variation of the diffusion coefficients is of the order of

Table 3
Viscosity of some common solvents

	Temperature (°C)	Dynamic viscosity, η (cP)	α ($\times 10^3$)	Density, ρ (kg/L)	Kinematic[a] viscosity, μ
n-Pentane	30	0.220	1.06	0.619	0.355
n-Hexane	30	0.296	1.15	0.657	0.450
n-Heptane	30	0.355	1.09	0.678	0.523
n-Octane	30	0.483	1.12		
Benzene	30	0.566	1.22	0.872	0.649
Chloroform	30	0.519	0.625	1.466	0.354
Carbon tetrachloride	30	0.845	1.25	1.582	0.534
Diethyl ether	20	0.212	1.11	0.716	0.296
Acetone	30	0.285	0.684	0.783	0.363
Methyl acetate	30	0.390	0.810		
Methanol	20	0.520	0.470	0.779	0.66
Ethanol	20	1.003	0.585	0.794	1.26
Water	0	1.79	−0.080	0.9998	1.79
Water	10	1.29	−0.046	0.9997	1.29
Water	30	0.80	0.053	0.9956	0.80
Water	75	0.38	0.076	0.9749	0.39
Acetonitrile	30	0.324	0.624	0.7711	0.42

[a] Unit: 1 centistoke = 1×10^{-2} cm^2 s^{-1}.

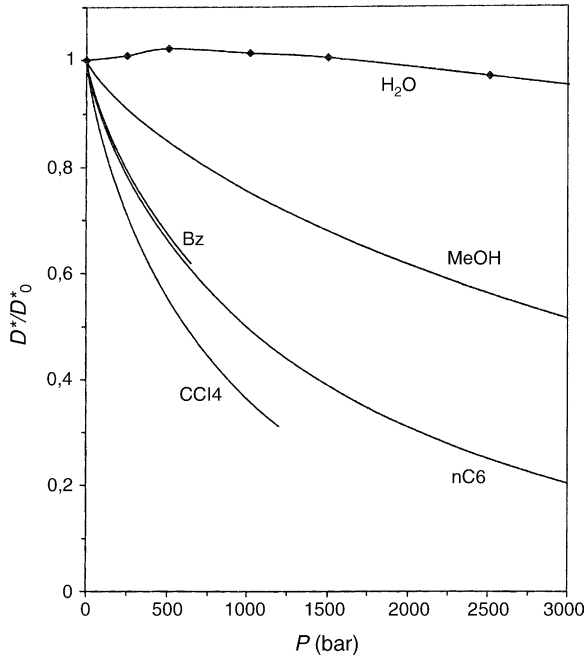

Fig. 4. Ratio of the self-diffusion coefficient, D^*, to the self-diffusion coefficient under atmospheric pressure, D_0^*, vs. the pressure, P, for various liquids at 25 °C. *Symbols*: CCl_4, carbon tetrachloride; *n*C6, *n*-hexane; Bz, benzene; MeOH, methanol; H_2O, water. The curve for water was drawn from experimental data points [27]. The curves are limited to the pressure domain within which the empirical parameters of Eq. (11), χ and m have been determined.

$1 \times 10^{-3}\,\text{bar}^{-1}$, may be even more for large molecules, e.g., proteins. This means that, at a constant flow rate, the reduced velocity is not constant along a column. This observation was used to explain why the column efficiency increases often more slowly than the number of identical columns connected in series [28], a result recently confirmed by Ikegami et al. in their investigations of the efficiencies of assemblies of monolithic columns [29]. Also, it shows that the coefficients of a plate height equation derived by fitting experimental data differ significantly from their local values. The errors made can be quite significant under conventional conditions, up to 100% for the coefficient C of a van Deemter equation [28]. This result is similar to those observed long ago in gas chromatography [30] and in thin-layer chromatography [31].

In the pressure range considered here, the pressure effect would be so large as to render meaningless the values of the coefficients of a plate height equation derived from elution band profiles that integrate the influence of the pressure on the mass transfer coefficients over the huge range of pressures experienced by the band during its migration. This conclusion is consistent with recent results that showed very high values of the C term of the reduced van Deemter plate height equation measured with a maximum inlet pressure of 6800 bar [32]. The interpretation of these results is far more complex than empirical experimentalists may believe because the reduced plate heights that they measured do not correspond to any single value of the reduced velocity but to an average value of this velocity: since the diffusion coefficient varies along the column, so does the reduced velocity. The range of reduced velocity over which the averaging is performed changes for each point of a van Deemter plot. The classical approach relating local and average plate heights should be followed to account for these results [30,31].

2.5. Influence of pressure on equilibrium constants in diphasic systems

Some fundamental relationships of thermodynamics, which arise from the definitions of the basic functions, energy, U, enthalpy, H, entropy, S, and Gibbs free energy, G, of a system are

$$H = U + PV \tag{12a}$$

$$G = H - TS = U + PV - TS \tag{12b}$$

where P, V, and T are the pressure, the volume and the temperature of the system, respectively. Differentiation of Eq. (12) at constant volume with respect to pressure shows that

$$\frac{\partial G}{\partial P} = V \tag{13}$$

We know that the equilibrium constant in a biphasic system is given by

$$K = \frac{C_\text{s}}{C_\text{m}} \tag{14a}$$

$$\Delta G = -RT\ \ln\ K \tag{14b}$$

where C_s and C_m are the equilibrium concentrations of the solute considered in the stationary and the mobile phases, respectively, and ΔG is the change in Gibbs free energy associated with the passage of a mole of solute from the mobile to the stationary phase. Accordingly, we obtain

$$\frac{\partial \Delta G}{\partial P} = -RT\,\frac{\partial \ln\ K}{\partial P} = \Delta V \tag{15}$$

where ΔV is the change of partial molar volume associated with the adsorption of the solute [33,34].

The retention factor is the product of the equilibrium constant and the phase ratio. If we neglect the dependence of the phase ratio on the local pressure (because the effects are moderate, we may account separately for the influence of pressure on the phase ratio and the equilibrium constant), the dependence of the retention factor on the pressure is given by

$$\frac{\partial \ln k'}{\partial P} = -\frac{\Delta V}{RT} \tag{16}$$

This equation assumes implicitly that a single retention mechanism accounts for the interactions of the solute in the phase system. This is not always the case. The retention of a compound may be the result of the combination of two or several

different retention mechanisms. If this is the case, the pressure dependence of k' is more complex than indicated by Eq. (16). A similar problem is encountered in the study of the influence of the temperature on the retention factors. Cases are known in which the results do not follow a simple van't Hoff relationship [35].

The pressure influence on the retention factor is illustrated in Fig. 5 where are plotted curves showing the variations of the ratio of the retention factor under pressure P, k', to the retention factor under atmospheric pressure, k'_0, versus P, for various values of ΔV, according to Eq. (16). The importance of the change of the partial molar volume of the solute associated with its adsorption is somewhat correlated with its size [36], so, according to Eq. (15), the pressure dependence of the retention factor of large molecular weight solutes will be much larger than that of small molecular weight ones (see [36] and later, Fig. 6). Thus, for a small-size protein like insulin, ΔV is of the order of -100 ml/mol and the retention factor doubles when the average pressure increases from 50 to 250 bar [34,36]. The corresponding values for lysozyme are slightly larger [37]. Smaller values were reported for *n*-decane and *n*-eicosane the retention factors of which increase by 9 and 24%, respectively, when the pressure increases from 100 to 350 bar [38]. Tanaka et al. [39] reported that the retention factor of nitro-phenol increases by 13% for an increase of the average pressure of 150 bar. Recently, Patel et al. [32] reported that the retention factor of 4-methyl catechol increases linearly with increasing pressure up to 6800 bar.

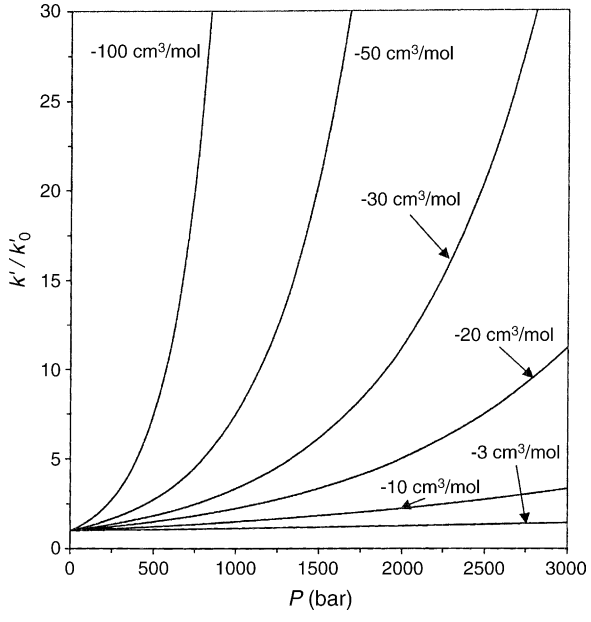

Fig. 5. Ratio of the retention factor, k', under pressure P to the retention factor under atmospheric pressure, k'_0. Plot of k'/k'_0 versus P, according to Eq. (16) for various values of the change in partial molar volume, ΔV, associated to the transfer of one mole of solute from the mobile to the stationary phase at 25 °C.

Since the variation of $\ln k'$ with the pressure is linear, and since, under the conditions of the experiments carried out by Szabelski et al. [34], Liu et al. [36], and Tanaka et al. [39], the compressibility of the mobile phase is practically negligible, the values measured, which are average values over the range of experimental conditions are equal to the value measured at the average column pressure [36]. This would no longer be true for measurements carried out under very large pressure gradients. The retention factors will then become functions of the flow rate—since it is impossible to change the flow rate without adjusting the pressure gradient accordingly. The separation factors of molecules of sizes or structures that are significantly different will change when the column inlet pressure varies. Finally, one should note that the measurements of thermodynamic properties, e.g., of the enthalpy of the retention mechanism, will have to be made at constant inlet pressure, in order to reduce the influence of the pressure gradient on the results [36]. This procedure would allow the complete separation of the influences of the temperature and the pressure (since the mobile phase viscosity is a function of the temperature, operating at constant flow rate affects the pressure gradient along the column) in the low pressure range. The effect is still more complex at high pressures.

Most investigations of the effects of pressure on retention data in HPLC were obtained at relatively low pressures, i.e., 50–300 bar. The results of measurements made years ago by Rogers and co-workers [40–42] at pressures up to 3500 bar showed that changes in the retention factors can exceed 300% and that they are accompanied by shifts in the elution orders. This suggests that chromatographic results recorded with columns operated under extremely high pressures will be far more difficult to account for than those of the traditional "low" pressure version of HPLC.

2.6. Influence of pressure on the dimensions of the column

Pressure affects the external and the internal dimensions of the column since the tube is subject to a stress that tends to inflate it and to increase its length, assuming that the column is closed at both ends by metal plugs through which only a narrow capillary tube of negligible internal cross-section area carries the mobile phase in and out the column. Because the column is operated with a finite mobile phase velocity, the inlet and outlet pressures are different and the column, that is initially cylindrical when the internal and external pressures are the same, takes the shape of a cone with a small angle. The calculation of the column dimensions under pressure is somewhat complicated because a significant pressure gradient exists along the column. As a first approximation, this gradient can be considered as constant (i.e., the longitudinal pressure profile is linear). Furthermore, we consider only safe, routine operations, in which case the column deformations are small and elastic. Then, the deformations

caused by the relatively small effects considered here take place in the elastic domain and are linearly related to the stresses applied which, themselves, are proportional to the local pressure difference between the inside and the outside of the column. Hence, under these conditions, the overall changes in the column internal volume and in the volume of the column tube itself are the same as those which would be observed if the pressure inside the column was constant and equal to the pressure, P_m, at mid length of the column.

Pressure also compresses the stationary phase. The effect is markedly different whether the column is packed with neat silica particles (the compressibility of silica is negligible) or with bonded alkyl-silica (the compressibility of the bonded layer, like that of fluids is far from negligible [43]). The combination of these two mechanical effects tends to increase the column porosity and its permeability since both act in the same direction, toward an increase in the geometrical column volume. It also affects the hold-up volume [43]. Obviously, in a chromatographic column, the local effects vary with the abscissa and the overall effect will be the integral of these local effects.

Let L_0, $r_{in,0}$, and $r_{ext,0}$ be the length, the internal and the external radius of the cylindrical tubular column when the internal and the external pressures are both equal to P_0, the reference and, in the general case, the atmospheric pressure. In the following, we assume that the internal pressure is equal to P_m, and that the external pressure, as well as the column outlet pressure are equal to P_0. Then, one has:

$$p_m = P_m - P_0 = \frac{\Delta P}{2} \tag{17}$$

where ΔP is the pressure drop along the chromatographic column.

2.6.1. General equations for elastic materials

Two different approaches are used in solid mechanics, those due to Young and to Lamé [44–46]. We use the former here.

2.6.1.1. Young formalism. The Young formalism gives the following relationships between stresses and deformations of elastic materials [44–46]:

$$E\bar{\epsilon} = -\eta Tr(\bar{\sigma})\bar{\delta} + (1+\eta)\bar{\sigma} \tag{18}$$

where $\bar{\epsilon}$ is the relative deformation tensor, $\bar{\sigma}$ the stress tensor, $\bar{\delta}$ the unit tensor, E the Young modulus, and η is the Poisson coefficient of the material. $Tr(\bar{t})$ is the trace of the tensor $\bar{t}$, i.e., the sum of its diagonal elements. When the stresses are acting along the principal axes of the material (for instance, z, r, and θ, the axial, the radial, and the tangential directions in a cylindrical geometrical reference system), there is no shear stress in the material. Therefore, the non-diagonal elements of the deformation and of the stress tensors vanish and Eq. (18) reduces to the three following fundamental equations

$$E\epsilon_r = -\eta(\sigma_r + \sigma_\theta + \sigma_z) + (1+\eta)\sigma_r = \sigma_r - \eta(\sigma_\theta + \sigma_z) \tag{19a}$$

$$E\epsilon_\theta = \sigma_\theta - \eta(\sigma_r + \sigma_z) \tag{19b}$$

$$E\epsilon_z = \sigma_z - \eta(\sigma_\theta + \sigma_r) \tag{19c}$$

η is typically equal to 1/3 for metals, the range of variations of η being from about 0 for cork to 1/2 for rubber.

2.6.1.2. Relative deformations and displacements in a cylindrical geometry. Let s be the radial displacement of a point which was originally at distance r from the cylinder (i.e., column) axis. Simple geometrical considerations show that the relative deformations along the radial and the tangential directions are equal to

$$\epsilon_r = \frac{\partial s}{\partial r} \tag{20a}$$

$$\epsilon_\theta = \frac{s}{r} \tag{20b}$$

In the following, the combination of Eqs. (19b) and (20b) gives the radial displacement, s since we have

$$s = r\epsilon_\theta = \frac{r}{E}[\sigma_\theta - \eta(\sigma_r + \sigma_z)] \tag{21}$$

The variation of the column length is derived from Eq. (19c), as

$$h = \epsilon_z L_0 = \frac{L_0}{E}[\sigma_z - \eta(\sigma_\theta + \sigma_r)] \tag{22}$$

2.6.2. Determination of the stresses

In the following, we assume that the stresses exerted on the column tube arise solely from the effects of the pressure differences across the internal and external sides of the tube and on the extremities of the tube, i.e., that the column is free to deform itself as a consequence of these sole stresses. Furthermore, we recognize that, in practice, the nuts closing the column ends are strong enough to limit the deformations at the extremities, so that, under a uniform inside pressure, the column will somewhat look like a barrel rather than a cylinder. We will assume these deformations to be negligible. The effects of the column ends are neglected in this review. Solid mechanics has now computer programs that can account for far more complex boundary conditions.

2.6.2.1. Determination of the radial and tangential stresses. Far away from the extremities of the cylinder, the distribution of the deformations in the radial and tangential directions can be considered as independent of z, according to the principle of De Saint-Venant [46]. For thin cylinders, the error on the estimates of the deformations that arise from this approximation is lower than 0.3% at a distance from the bases that is larger than $\pi\sqrt{2r_{in,0}(r_{ext,0} - r_{in,0})}$ [46]. Then, a balance

of the forces acting on the four sides of an element of the cross-section of the solid wall between radii r and $r + dr$ and between the angles θ and $\theta + d\theta$ leads the following relationship

$$\sigma_\theta - \sigma_r - r\frac{\partial \sigma_r}{\partial r} = 0 \tag{23}$$

In the general case, when the internal and external pressures are $p_{in} + P_0$ and $p_{ext} + P_0$, respectively (P_0 being the pressure at which the cylinder dimensions are measured, at rest, i.e., at the atmospheric pressure), the boundary conditions are

$$\sigma_r(r_{in,0}) = -p_{in} \tag{24a}$$

$$\sigma_r(r_{ext,0}) = -p_{ext} \tag{24b}$$

Note that, by convention, a minus sign is used for compression stresses.

Suitable manipulations of Eqs. (19)–(24) allow the derivation of the relationships between the radial and tangential stresses and the internal and external radii of the tube [44–46]

$$\sigma_r(r) = \frac{r_{in,0}^2 p_{in} - r_{ext,0}^2 p_{ext}}{r_{ext,0}^2 - r_{in,0}^2} - \frac{r_{in,0}^2 r_{ext,0}^2}{r^2\,(r_{ext,0}^2 - r_{in,0}^2)}(p_{in} - p_{ext}) \tag{25a}$$

$$\sigma_\theta(r) = \frac{r_{in,0}^2 p_{in} - r_{ext,0}^2 p_{ext}}{r_{ext,0}^2 - r_{in,0}^2} + \frac{r_{in,0}^2 r_{ext,0}^2}{r^2\,(r_{ext,0}^2 - r_{in,0}^2)}(p_{in} - p_{ext}) \tag{25b}$$

These equations are general in the sense that they are valid whether $p_{in} < p_{ext}$ or $p_{in} > p_{ext}$, for tube walls working under expansion or compression.

In the case of interest in chromatography, the inner and outer pressures are P_m and P_0, i.e., $p_{in} = p_m$ and $p_{ext} = 0$, respectively, and one gets

$$\sigma_r(r) = \frac{r_{in,0}^2}{r_{ext,0}^2 - r_{in,0}^2} p_m \left(1 - \frac{r_{ext,0}^2}{r^2}\right) \tag{26a}$$

$$\sigma_\theta(r) = \frac{r_{in,0}^2}{r_{ext,0}^2 - r_{in,0}^2} p_m \left(1 + \frac{r_{ext,0}^2}{r^2}\right) \tag{26b}$$

The boundary conditions given in Eqs. (24a) and (24b) are consistent with Eq. (26a) (i.e., if $r = r_{ext,0}$ or $r = r_{in,0}$).

2.6.2.2. Determination of the axial stress. The force, F, exerted by the pressure inside the column on the fitting holding this column is

$$F = p_m S_{in,eff} \tag{27}$$

where $S_{in,eff}$ is the effective column cross-sectional area, on which the pressure differential, p_m, is exerted inside the chromatographic column. Because the inlet pressure is exerted on both sides of the frit on the central part of the frit corresponding to the cross-section of the incoming tube of radius r_t, one gets:

$$S_{in,eff} = \pi r_{in,0}^2 (1 - k) \tag{28a}$$

with

$$k = \left(\frac{r_t}{r_{in,0}}\right)^2 \tag{28b}$$

Note that in most practical cases, k is negligible, being smaller than 0.01. This force is transmitted, through the fitting, onto the material making the annular cross-section of the tube. The resulting longitudinal stress, σ_z, is then:

$$\sigma_z = p_m \frac{r_{in,0}^2}{r_{ext,0}^2 - r_{in,0}^2}(1 - k) \tag{29}$$

2.6.3. Column deformation

The radial displacement, $s(r)$, of a point at distance r from the axis is obtained from Eq. (21), together with the expressions of the stresses given by Eqs. (26) and (29), as:

$$s(r) = r\frac{r_{in,0}^2}{r_{ext,0}^2 - r_{in,0}^2}\frac{p_m}{E}\left[1 + \frac{r_{ext,0}^2}{r^2} - \eta\left(2 - \frac{r_{ext,0}^2}{r^2} - k\right)\right] \tag{30}$$

The relative changes of the inner and outer radii of the column are thus given by

$$\frac{s(r_{in})}{r_{in,0}} = \frac{r_{in,0}^2}{r_{ext,0}^2 - r_{in,0}^2}\frac{p_m}{E}\left[(1 - 2\eta + \eta k) + (1 + \eta)\frac{r_{ext,0}^2}{r_{in,0}^2}\right] \tag{31a}$$

$$\frac{s(r_{ext})}{r_{ext,0}} = \frac{r_{in,0}^2}{r_{ext,0}^2 - r_{in,0}^2}\frac{p_m}{E}(2 - \eta + \eta k) \tag{31b}$$

The change in the column length is obtained by combining Eqs. (22), (25), (26), and (29), as

$$h = \frac{p_m}{E}\frac{r_{in,0}^2}{r_{ext,0}^2 - r_{in,0}^2}(1 - 2\eta - k)L_0 \tag{32}$$

This equation shows that the change in column length is independent of the radius r, hence the bases remain flat and perpendicular the the column axis.

2.6.4. Column dimensions under pressure

We derive first the general equations, then a simplified set of equations valid for stainless steel columns in the case in which the cross-section areas of the tubings connecting the column to the equipment are negligibly small.

2.6.4.1. General case. In the general case of a connecting tube of finite diameter, the dimensions of the column tube

submitted to a pressure $p_m + P_0$ inside and P_0 outside are easily obtained from these equations as

$$\frac{r_{in}}{r_{in,0}} = 1 + \frac{s(r_{in})}{r_{in,0}} = 1 + \frac{r_{in,0}^2}{r_{ext,0}^2 - r_{in,0}^2} \times \left[1 + \frac{r_{ext,0}^2}{r_{in,0}^2} + \eta\left(\frac{r_{ext,0}^2}{r_{in,0}^2} + k - 2\right)\right]\frac{p_m}{E} \quad (33a)$$

$$\frac{r_{ext}}{r_{ext,0}} = 1 + \frac{s(r_{ext})}{r_{ext,0}} = 1 + \frac{r_{in,0}^2}{r_{ext,0}^2 - r_{in,0}^2}[2 - \eta(1-k)]\frac{p_m}{E} \quad (33b)$$

$$\frac{L}{L_0} = 1 + \frac{h}{L_0} = 1 + \frac{r_{in,0}^2}{r_{ext,0}^2 - r_{in,0}^2}(1 - 2\eta - k)\frac{p_m}{E} \quad (33c)$$

Since η is smaller than 0.5 and k is very small, Eqs. (33a) to (33c) show that the inner radius, the outer radius and the column length all increase with increasing inner pressure.

The tube wall thickness changes from e_0 to e, such that

$$e = e_0 + s(r_{ext,0}) - s(r_{in,0}) \quad (34)$$

or

$$\frac{e}{e_0} = 1 - \frac{r_{in,0}^2}{r_{ext,0}^2 - r_{in,0}^2}\left[(1+\eta)\frac{r_{ext,0}}{r_{in,0}} - (1 - 2\eta + \eta k)\right]\frac{p_m}{E} \quad (35)$$

Since η is smaller than 1/2, and $r_{ext,0}$ is larger than $r_{in,0}$, Eq. (35) shows that the thickness of the column tube decreases with increasing inner pressure, i.e., that its inner radius increases faster than its outer radius.

The cross-sectional area of the tube changes also, from $S_{t,0}$ to S_t, so that

$$\frac{S_t}{S_{t,0}} = \frac{r_{ext}^2 - r_{in}^2}{r_{ext,0}^2 - r_{in,0}^2} = 1 + \frac{2r_{in,0}^2}{r_{ext,0}^2 - r_{in,0}^2}(1 - 2\eta + \eta k)\frac{p_m}{E} \quad (36)$$

when neglecting the higher degree terms in $(p_m/E)^2$. The equation shows that the cross-sectional area of the tube increases with increasing pressure although its thickness decreases.

Finally, from Eqs. (33) and (36), it appears that the change in the column volume, from $V_{t,0}$ to V_t, is given by

$$\frac{V_t}{V_{t,0}} = \frac{LS_t}{L_0 S_{t,0}} = 1 + \epsilon_r + \epsilon_\theta + \epsilon_z = 1 + \frac{1-2\eta}{E}(\sigma_r + \sigma_\theta + \sigma_z) = 1 + \frac{r_{in,0}^2}{r_{ext,0}^2 - r_{in,0}^2}(1-2\eta)(3-k)\frac{p_m}{E} \quad (37)$$

As both the cross-sectional area and the length of the column tube increase under increasing pressure, its volume also increases. This implies that the density of the tube material decreases. This result might seem shocking since the changes of the tube dimensions arise from the application of a pressure inside the tube. In fact, it reflects the great importance of the tangential (or circumferential) stress that is caused by the inside pressure, through stretching of the atoms of the tube material.

The column cross-sectional area of the tube changes also under pressure, from $S_{c,0}$ to $S_c = \pi r_{in}^2$, such that

$$\frac{S_c}{S_{c,0}} = (1 + ap_m)^2 \quad (38a)$$

with

$$a = \left[(1 - 2\eta + \eta k) + (1+\eta)\frac{r_{ext,0}^2}{r_{in,0}^2}\right]\frac{r_{in,0}^2}{r_{ext,0}^2 - r_{in,0}^2}\frac{1}{E} \quad (38b)$$

where a represents the relative increase of the column inner radius per unit of pressure drop across the column tube. A first-order expansion in p_m/E gives the following expression of the column inner volume

$$\frac{V_c}{V_{c,0}} = \frac{S_c}{S_{c,0}}\frac{L}{L_0} = 1 + \frac{(1-2\eta)(3-k)r_{in,0}^2 + 2(1+\eta)r_{ext,0}^2}{r_{ext,0}^2 - r_{in,0}^2}\frac{p_m}{E} \quad (39)$$

where $V_{c,0}$ is the internal volume of the column at rest or its geometrical volume. Since both the inner radius and the column length increase under increasing pressure, the column volume also increases.

2.6.4.2. Simplified equations. In the particular case of a stainless steel column connected with inlet tubings of negligible cross-section, Eqs. (33)–(39) simplify. For stainless steel, η is equal to 1/3. For inlet tubings of negligible cross-section (i.e., $r_{ext,0}/r_{in,0} < 0.1$), k is equal to 0. Then, one obtains the following geometrical characteristics of the tube, from Eqs. (33a), (33b), (33c), (35), (36) and (37):

$$\frac{r_{in}}{r_{in,0}} = 1 + \left(\frac{1}{3} + \frac{4}{3}\frac{r_{ext,0}^2}{r_{in,0}^2}\right)\frac{r_{in,0}^2}{r_{ext,0}^2 - r_{in,0}^2}\frac{p_m}{E} \quad (40a)$$

$$\frac{r_{ext}}{r_{ext,0}} = 1 + \frac{5}{3}\frac{r_{in,0}^2}{r_{ext,0}^2 - r_{in,0}^2}\frac{p_m}{E} \quad (40b)$$

$$\frac{L}{L_0} = 1 + \frac{1}{3}\frac{r_{in,0}^2}{r_{ext,0}^2 - r_{in,0}^2}\frac{p_m}{E} \quad (40c)$$

$$\frac{e}{e_0} = 1 - \left(\frac{4}{3}\frac{r_{ext}}{r_{in,0}} - \frac{1}{3}\right)\frac{r_{in,0}^2}{r_{ext,0}^2 - r_{in,0}^2}\frac{p_m}{E} \quad (40d)$$

$$\frac{S_t}{S_{t,0}} = 1 + \frac{2}{3}\frac{r_{in,0}^2}{r_{ext,0}^2 - r_{in,0}^2}\frac{p_m}{E} \quad (40e)$$

$$\frac{V_t}{V_{t,0}} = 1 + \frac{r_{in,0}^2}{r_{ext,0}^2 - r_{in,0}^2}\frac{p_m}{E} \quad (40f)$$

where S_t and V_t are the cross-section area and the volume of the metal in the tube.

Typically, for stainless steel tubes, E is equal to 200 GPa, i.e. to 2×10^6 bar. If the $r_{ext,0}/r_{in,0}$ ratio is equal to 2, the relative increase of the column length is 0.0028%/kbar of pressure drop along the column, i.e., an increase of 2.8 μm/kbar for a 10 cm long column (NB. A 1 kbar pressure drop along the column means that $p_m = 500$ bar). The mean increase of the internal radius is 0.047%/kbar and that of the internal volume is 0.097%/kbar.

It appears that the contribution of the variation of the column length to the change in the column volume is 34 times smaller than that of the column cross-sectional area. When the ratio of the external to the internal radius becomes larger than 2, the change in column length vanishes and the limit value of the change in the column volume is $8p_m/3E$, or, typically, 0.067%/kbar of pressure drop along the column. Accordingly, when, in the following, an integration with respect to the distance along the column is performed, the column length will be considered as constant.

The variations of the ratio $S_c/S_{c,0}$ versus the pressure of the column, $P = p_m + P_0$, are shown in Fig. 6 for different values of the ratio of the outer to the inner column radii, $r_{ext,0}/r_{in,0}$.

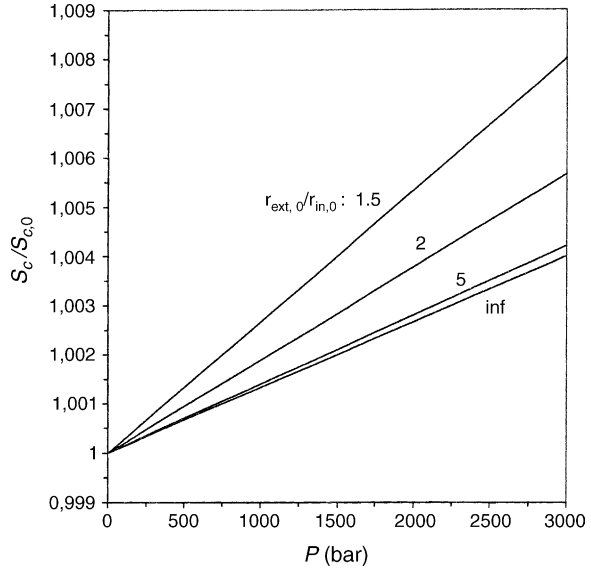

Fig. 6. Ratio of the column cross-sectional area, S_c, under inner pressure P, to the column cross-sectional area under atmospheric pressure, $S_{c,0}$, vs. P, for various values of the ratio of the inner and outer column radii, $r_{ext,0}/r_{in,0}$. Young modulus, $E = 2$ GPa; $k = 0$.

2.6.5. Rupture of the tube under pressure

As a result of the stress applied by the inner pressure on the inner wall of the tube, the column wall undergoes a circumferential traction stress, σ_θ. This stress decreases with increasing value of r, as shown by Eq. (26b). It is thus maximum at the inner wall, where it is equal to

$$\sigma_\theta = \frac{r_{ext,0}^2 + r_{in,0}^2}{r_{ext,0}^2 - r_{in,0}^2} p_m \quad (41a)$$

If σ_M is the resistance of the tube material to traction, i.e., is the maximum stress that can be exerted before an immediate rupture takes place, the maximum inlet pressure that can be applied to the column before rupture is given by

$$p_{m,M} = \frac{r_{ext,0}^2 - r_{in,0}^2}{r_{ext,0}^2 + r_{in,0}^2}\sigma_M \quad (41b)$$

Hence $p_{m,M} = 0.6\sigma_M$ for $r_{ext,0}/r_{in,0}$ equal to 2. The value of σ_M depends on the type of steel used. It is around 10 kbar for medium resistance steels and can reach over 20 kbar for high resistance steels.

One should note that these values of σ_M correspond to the rupture of the material. When the traction stress is small, the material undergoes reversible deformations. This is the elastic domain. Above a certain stress threshold, σ_{el}, the deformations become irreversible. This is the plastic domain, which ends up at σ_M, by the rupture of the material. The value of σ_{el} also depends on the nature of the tube material, but it is generally of the order of $\sigma_M/2$.

2.7. Influence of the pressure on the column characteristics

The change in the column dimensions will affect column characteristics that are important in chromatography, the porosity and the permeability of the column.

2.7.1. Pressure dependence of the column porosity

A chromatographic column is always packed before it is used. The manufacturing of chromatographic columns includes a consolidation step during which the column bed is percolated at high flow rate by a solvent compatible with the packing material. In order to prepare stable columns that will have a long life time, their consolidation is achieved by pumping this solvent stream at a pressure that exceeds the maximum pressure at which the column will be used later. During this consolidation, the column tube expands as explained in the previous section. At the end of this step, the column is entirely filled with packing material. When the stream is stopped, the column tube shrinks back. The bed is compressed elastically. A part of it might be expelled, depending on the friction between the column tube and the bed. The operation of relaxing the pressure and closing the column must be carefully made, under conditions that minimize this expulsion. When the inlet frit is in place, the packing remains under compression. When the pressure is raised again at the

column inlet, to operate the column, the tube expands and the packing compression decreases. The bed is elastic, however, and the bed remains stable as long as the inlet pressure does not exceed the packing pressure. As a result of the pressure applied and the bed elasticity, the column porosity and its permeability will increase somewhat with increasing pressure. The results of recent measurements performed under very high pressures, up to 4600 [22] and 6800 [32] bar confirmed this analysis. The packing material must be consolidated at a pressure exceeding the highest inlet pressure under which the column must be run.

The total porosity increases with increasing pressure because (1) the volume of the solid packing in a slice of column of length δz decreases slightly with increasing pressure, due to the slight compressibility of the solid packing, and (2) the column volume increases in proportion to the cross-section area (see previous section). Let β be the compressibility of the bed of packing material:

$$\beta = -\frac{1}{\delta V_s}\frac{\mathrm{d}(\delta V_s)}{\mathrm{d}P} \tag{42}$$

where δV_s is the volume of packing material contained in the slice of length δz. Assuming that β is independent of the local pressure, integration of this equation gives:

$$\delta V_s = \delta V_{s,0}\mathrm{e}^{-\beta(P-P_0)} \tag{43}$$

where $\delta V_{s,0}$ is the volume of the same mass of packing at the reference pressure, P_0. Assuming that the mass of solid in the slice of length δz is not affected by the pressure (and that the slice length as well as the column length are not affected by pressure changes), the total porosity in the slice is equal to:

$$\epsilon_t = \frac{S_c\delta z - \delta V_s}{S_c\delta z} = 1 - \frac{\delta V_s}{S_c\delta z} \tag{44}$$

Let S_c and $S_{c,0}$ be the column cross-sectional areas at pressures P and P_0, respectively. Combining Eqs. (38a), (43), and (44), and noting that the total porosity at the reference pressure is equal to:

$$\epsilon_{T,0} = 1 - \frac{\delta V_{s,0}}{S_{c,0}\delta z} \tag{45}$$

gives the pressure dependence of the total porosity:

$$\epsilon_t = 1 - (1-\epsilon_{T,0})\frac{\mathrm{e}^{-\beta(P-P_0)}}{[1+a(P-P_0)]^2} \tag{46}$$

where a is given by Eq. (38b), after substitution of p_m by $P - P_0$, where P is the local pressure in Eq. (38a), i.e., for a metal tube, according to Eq. (40a)

$$a = \left[\frac{1}{3} + \frac{4}{3}\frac{r_{ext,0}^2}{r_{in,0}^2}\right]\frac{r_{in,0}^2}{r_{ext,0}^2 - r_{in,0}^2}\frac{1}{E} \tag{47}$$

2.7.2. Pressure dependence of the column permeability

The permeability, k, of a bed packed with particles of diameter d_p is given by the Blake–Kozeny equation:

$$k = \frac{d_p^2}{150}\frac{\epsilon_e^3}{(1-\epsilon_e)^2}\frac{1}{\epsilon_t} \tag{48}$$

where ϵ_e is the extra-particle porosity. If the particles are non-porous, ϵ_t, given by Eq. (46), becomes equal to ϵ_e and will be simply denoted ϵ in the following and ϵ_0 is the porosity at the reference pressure, P_0. k becomes:

$$k = \frac{d_p^2}{150}\frac{\epsilon^2}{(1-\epsilon)^2} \tag{49}$$

The compression of the particles in the bed being isotropic, the change in their diameter with increasing pressure can be expressed as:

$$d_p = d_{p,0}\mathrm{e}^{-\beta(P-P_0)/3} \tag{50}$$

where $d_{p,0}$ is the particle diameter under the reference pressure P_0. Let k_0 be the permeability under pressure P_0 and combine the previous equations (Eqs. (46), (49), and (50)). This gives the pressure dependence of the permeability as:

$$k = \frac{k_0}{\epsilon_0^2}\langle[1+a(P-P_0)]^2 - (1-\epsilon_0)\mathrm{e}^{-\beta(P-P_0)}\rangle^2\mathrm{e}^{4\beta(P-P_0)/3} \tag{51}$$

The local permeability varies along the column. Because the effects of the pressure remain moderate, a first-order Taylor expansion of this equation will capture the essential of the effect

$$\frac{k}{k_0} = 1 + (P-P_0)\left[\frac{4a}{\epsilon_0} + \left(\frac{2}{\epsilon_0} - \frac{2}{3}\right)\beta\right] \tag{52}$$

Since the coefficients a and β are positive and ϵ_0 is smaller than 1, the permeability increases always with increasing pressure, at a relative rate of $1.3 \times 10^{-5}\,\mathrm{bar}^{-1}$, assuming the values given above for the change in column radius, a value of $1 \times 10^{-6}\,\mathrm{bar}^{-1}$ for the compressibility of the solid packing material, and a value of 0.4 for ϵ_0. This leads to a 1.3% decrease of the pressure gradient for an increase of 1 kbar of the local pressure. Note that, according to Eq. (52), k is the sum of two terms, the (positive) contribution of the column porosity that increases with increasing pressure and the (negative) contribution of the particle size due its compressibility, that decreases with increasing pressure. Their combined effects add up.

2.8. Influence of pressure on the pressure profile, the flow rate and the elution characteristics

It would not be very useful to discuss separately each of the previous effects. They combine and cannot reasonably be separated for detailed studies. The column dimensions expand under increasing pressure, the mobile phase is compressed and its viscosity increases. All these effects combine

and affect the pressure profile along the column, hence the gradient of linear velocity of the mobile phase. Finally, it is not possible to force a high velocity stream of liquid through a low permeability bed, as we do in HPLC, without generating a certain amount of heat due to the compressibility of the liquid and its friction against the bed. This heat effect has consequences that depend on the column diameter. They will be discussed in a later section.

Conventional HPLC instruments are designed to pump the mobile phase into the column at a constant flow rate. Under steady-state conditions, the pump delivers a constant mass flow rate of carrier liquid and this mass flow rate is constant all along the column, which expresses the conservation of the mass of this carrier. Let $\dot{m}$ represent the mass of mobile phase flowing through the column cross-section per unit time. To the mass flow rate corresponds a volumetric flow rate, Q, which is the volume of mobile phase flowing through a column cross-section per unit time. The parameters $\dot{m}$ and Q are related by

$$\dot{m} = \rho Q \tag{53}$$

where ρ is the mass per unit volume of the mobile phase (which will be later called, for short, its density). Because ρ depends on the local pressure, Q is not constant all along the column but it can be derived from Tait equation (Eqs. (4) and (5)) which gives the volume, V, occupied by a given mass of carrier as a function of the pressure, P, at a given temperature. If one considers that this mass is that flowing through the column per unit time, i.e., the mass flow rate, $\dot{m}$, then the volume V in Eq. (4) becomes the volumetric flow rate and

$$Q = Q_0 \left[1 + c \ln\left(\frac{P_0 + b}{P + b}\right)\right] \tag{54}$$

This flow rate is related to the cross-sectional average flow velocity, u, as:

$$Q = u\epsilon_t S_c \tag{55}$$

2.8.1. Darcy law and the basic fluid flow equation

Darcy law [48] expresses the proportionality between the cross-sectional average fluid velocity, u, and the pressure gradient, $\mathrm{d}P/\mathrm{d}z$, as:

$$u = -\frac{k}{\eta}\frac{\mathrm{d}P}{\mathrm{d}z} \tag{56}$$

Deviations from Darcy law behavior are noticed when the apparent Reynolds number, $ud_p\epsilon_e/[\mu(1-\epsilon_e)]$, is relatively large. A deviation of about 1.2% was reported at a value of this number of 1 [47]. In classical HPLC, however, with 4.6 mm i.d. columns packed with 10 μm particles and operated at a flow rate of 1 ml/min, this number is of the order of 1×10^{-2} (see Table 3 for typical μ values). In ultra high pressure LC with columns packed with particles having diameters as low as 1.5 μm and operated at velocities as large as 1 cm/s, the apparent Reynolds number is of the same order of magnitude. Hence, significant deviations from Darcy law behavior is improbable and the possible consequences of this effect will be neglected in the following.

Combining this equation with Eqs. (10), (46), (51), (54), and (55), gives:

$$\frac{u_0\eta_0}{k_0}\,\mathrm{d}z = -h(P)\,\mathrm{d}P \tag{57a}$$

with:

$$h(P) = \frac{\langle[1+a(P-P_0)]^2-(1-\epsilon_0)\mathrm{e}^{-\beta(P-P_0)}\rangle^3\mathrm{e}^{4\beta(P-P_0)/3}}{\epsilon_0^3\left[1+c\,\ln((P_0+b)/(P+b))\right]\,[1+\alpha(P-P_0)]} \tag{57b}$$

where u_0 is the cross-sectional average velocity of the mobile phase under the reference pressure P_0, and is given by:

$$u_0 = \frac{Q_0}{\epsilon_0 S_{c,0}} = \frac{Q_0 L}{\epsilon_0 V_{c,0}} \tag{58}$$

where L is the column length and $V_{c,0} = S_{c,0}L_0$, the geometrical volume of the empty column when it is under the uniform pressure P_0. It can be verified that if α, η, a and c are set equal to 0, $h(P)$ becomes equal to 1. In the following, the reference pressure, P_0, is selected to be the pressure at the column outlet, usually the atmospheric pressure.

Integrating the basic flow equation (Eq. (57a)) provides the relationship between the column inlet pressure, P_i, and the outlet mobile-phase flow-velocity, u_0 (or the outlet flow rate, Q_0):

$$\int_{P_0}^{P_i} h(P)\,\mathrm{d}P = u_0\frac{\eta_0 L}{k_0} = Q_0\frac{\eta_0}{\epsilon_0 k_0}\frac{L^2}{V_{c,0}} \tag{59}$$

Two particular cases are interesting to consider when one wants to compare the actual pressure–flow rate relationship with the one that would be obtained for a so-called "ideal" system, i.e., a system for which the mobile phase, the packing material, and the column wall material are incompressible, and, for which the carrier has a constant viscosity, independent of the local pressure. These cases correspond to the operation of the column at a constant outlet flow rate or under a constant inlet pressure. The results obtained in these two cases are derived below.

2.8.1.1. Operating the column at a selected outlet flow rate. If the instrument used allows the selection of the outlet flow rate, i.e., the setting of the flow rate measured at the column outlet, usually under atmospheric pressure, Eq. (59) allows the determination of the inlet pressure P_i that corresponds to this imposed outlet flow rate, Q_0. For the ideal system (for which $h(P) = 1$), the RHS of Eq. (59) represents the ideal pressure drop, ΔP_{id}, that would be needed in order to have the same flow rate:

$$\Delta P_{id} = u_0\frac{\eta_0 L}{k_0} = Q_0\frac{\eta_0}{\epsilon_0 k_0}\frac{L^2}{V_{c,0}} \tag{60}$$

which is different from the actual pressure drop obtained in this case, $\Delta P = P_i - P_0$.

2.8.1.2. Operating the column at a selected inlet pressure. If the instrument system allows the selection of the column inlet pressure, P_i, or equivalently, of the column pressure drop, ΔP, Eq. (59) allows the calculation of the actual flow rate, Q_0 or of the outlet flow velocity, u_0. From Eq. (59) we can derive that, when $h(P) = 1$, the outlet flow rate, $Q_{id,0}$, or the outlet flow velocity, $u_{id,0}$, that would be obtained for the same pressure drop, ΔP, with an ideal system, are such that:

$$\frac{u_0}{u_{id,0}} = \frac{Q_0}{Q_{id,0}} = \frac{\int_{P_0}^{P_i} h(P)\,dP}{P_i - P_0} \tag{61}$$

2.8.2. Pressure gradient and velocity

Integration of Eq. (57a) between the position z and the column outlet gives

$$\int_{P_0}^{P} h(P)\,dP = u_0 \frac{\eta_0(L-z)}{k_0} = Q_0 \frac{\eta_0}{\epsilon_0 k_0} \frac{L(L-z)}{V_{c,0}} \tag{62}$$

hence, in combination with Eq. (59), the pressure profile is given by

$$\frac{z}{L} = 1 - \frac{\int_{P_0}^{P} h(P)\,dP}{\int_{P_0}^{P_i} h(P)\,dP} \tag{63}$$

and the relative pressure gradient is

$$-\frac{dP/dz}{\Delta P/L} = \frac{\int_{P_0}^{P_i} h(P)\,dP}{(P_i - P_0)h(P)} \tag{64}$$

These last two equations give the relative pressure gradient (Eq. (64)) and the position along the column (Eq. (63)) as parametric expressions that are both functions of P. Their combination allows the determination of the pressure gradient along the column. The velocity profile of the mobile phase along the column can be derived using a similar combination of the equations above.

2.8.3. Pressure dependence of the hold-up time

The hold-up time, or elution time of an unretained solute, t_0, is obtained by integration along the column of the hold-up times in each successive column increment

$$dt_0 = \frac{dz}{u} \tag{65}$$

Combination of Eqs. (10), (46), (51), (54), (55), and (56) gives

$$t_0 = \frac{k_0}{u_0^2 \eta_0} \int_{P_0}^{P_i} g(P)\,dP \tag{66a}$$

with:

$$g(P) = \frac{\langle [1+a(P-P_0)]^2 - (1-\epsilon_0)e^{-\beta(P-P_0)}\rangle^4 e^{4\beta(P-P_0)/3}}{\epsilon_0^4 [1 + c\,\ln((P_0+b)/(P+b))]^2\,[1+\alpha(P-P_0)]} \tag{66b}$$

$$= h(P)\frac{[1+a(P-P_0)]^2 - (1-\epsilon_0)e^{-\beta(P-P_0)}}{\epsilon_0[1 + c\,\ln((P_0+b)/(P+b))]} \tag{66c}$$

These equations apply whatever the operating mode of the instrumental system. If one wants to compare this time to the hold-up time that would be observed with an ideal system (i.e., with an ideal liquid phase and column material), for which $g(P) = h(P) = 1$, one has to specify the exact operating mode. Using the two simple modes identified above we obtain the following results.

2.8.3.1. Operating the column at selected outlet flow rate. When operating the column with a selected, constant flow rate or velocity, u_0, the hold-up time, $t_{0,id,1}$ of the ideal liquid is given as L/u_0, or :

$$t_{0,id,1} = \frac{k_0}{u_0^2 \eta_0} \Delta P_{id} \tag{67}$$

and, according to Eqs. (59), (60), and (66a)

$$\frac{t_0}{t_{0,id,1}} = \frac{\int_{P_0}^{P_i} g(P)\,dP}{\int_{P_0}^{P_i} h(P)\,dP} \tag{68}$$

2.8.3.2. Operating the column at a selected inlet pressure. When the column is operated under constant, controlled inlet and outlet pressures, hence with a given value of ΔP, the hold-up time of the ideal liquid is

$$t_{0,id,2} = \frac{k_0 \Delta P}{u_{0,id}^2 \eta_0} = \frac{k_0 \Delta P}{u_0^2 \eta_0} \left(\frac{u_0}{u_{0,id}}\right)^2 \tag{69}$$

and, combining with Eqs. (61) and (66a)

$$\frac{t_0}{t_{0,id,2}} = \frac{(P_i - P_0)\int_{P_0}^{P_i} g(P)\,dP}{\left[\int_{P_0}^{P_i} h(P)\,dP\right]^2} \tag{70}$$

It is convenient to follow the same approach as did James and Martin [49] in their determination of the hold-up time in gas chromatography and to define a compressibility factor, j, such that:

$$j = \frac{L}{u_0 t_0} \tag{71}$$

Combining Eqs. (19), (66a), and (71) gives

$$j = \frac{\int_{P_0}^{P_i} h(P)\,dP}{\int_{P_0}^{P_i} g(P)\,dP} = \frac{t_{0,id,1}}{t_0} \tag{72}$$

Interestingly, j depends not only on the variables representing the pressure dependence of the mobile phase density (c and b) and of the elasticity of the packing material and the column tube, but also on the parameter accounting for the pressure dependence of the viscosity (α). This is obviously not the case for the James and Martin factor in gas chromatography (GC) since the viscosity of ideal gases does not depend on

their pressure (nor does that of actual gases used as carrier gases, under the low pressures needed in GC).

2.8.4. Hold-up volume, retention volumes, retention factors

The hold-up volume is defined as the volume of the mobile phase that exits from the column outlet during the hold-up time:

$$V_0 = Q_0 t_0 = u_0 \epsilon_0 S_{c,0} t_0 \tag{73}$$

Combining Eqs. (59), (66a), and (73), one gets

$$V_0 = V_{c,0}\epsilon_0 \frac{\int_{P_0}^{P_i} g(P)\,dP}{\int_{P_0}^{P_i} h(P)\,dP} \tag{74}$$

where $V_{c,0} = S_{c,0}L$ is the geometrical volume of the column in the absence of a pressure gradient. Comparison of Eqs. (68) and (74) shows that $V_0/(\epsilon_0 V_{c,0})$ is equal to $t_0/t_{0,id,1}$.

Because the retention volume in any slice of column is equal to the product of the local contribution to the hold-up volume, the local phase ratio, and the local retention constant, the retention volume is a complex function of the pressure.

2.9. Thermal effect

The reason to use chromatographic columns packed with very fine particles and to operate them at a high flow rate is to achieve fast analyses. It has been shown, however [50–52] that a solvent stream percolating through a column at a high velocity generates heat, due to the friction of the liquid against the surface of the particles. The compression of the solvent under high pressure in the pump also heats the solvent. The heat generated in the column or brought by the solvent diffuses across the bed to the column wall and toward the column compartment. Thus, temperature gradients appear in the column, in both the radial and the axial directions. In the most common case, the mobile phase pumped into a column is at a higher temperature than the column (because compression of the mobile phase is exothermic), the column center is warmer than the wall region, and the column exit is warmer than its inlet. Since the viscosity of liquids varies rapidly with their temperature, these thermal gradients cause corresponding gradients of velocity of the mobile phase. When the sample band is injected into the column, it is thin in the axial direction, nearly flat. If the radial distribution of velocities across the column is not flat, the band becomes warped and, at elution, it appears broader than it really is. The column efficiency decreases. Recent results have shown that the consequences of the thermal effect on the column efficiency may be minimized by using very narrow columns [32]. These effects do depend on the column diameter and seem to be practically negligible for columns having an inner diameter narrower than 0.15 mm. Nevertheless, the temperature of the mobile phase increases and the consequences of this thermal effect should be taken into account.

2.9.1. Basic thermodynamic relationships

Let consider a certain mass, m, of carrier liquid that occupies a volume V at temperature T and under pressure P and that undergoes an infinitesimally small transformation. During that transformation, a differential quantity of heat, dQ, is exchanged with the surroundings of the system. This heat exchange is associated with differential changes in the pressure, dP, in the temperature, dT, and in the volume, dV, such that [53a]

$$dQ = C_p\,dT + h\,dP \tag{75a}$$

$$dQ = C_V\,dT + l\,dV \tag{75b}$$

Note that dQ depends on only two of the three variables P, V, and T since these variables are related through an equation of state. C_P is the heat capacity at constant pressure, C_V, the heat capacity at constant volume. Writing dV as a total differential, we have

$$dV = \left(\frac{\partial V}{\partial T}\right)_P dT + \left(\frac{\partial V}{\partial P}\right)_T dP \tag{76}$$

Combining Eqs. (75) and (76) gives

$$\left[C_V + l\left(\frac{\partial V}{\partial T}\right)_P\right] dT + l\left(\frac{\partial V}{\partial P}\right)_T dP = C_p\,dT + h\,dP \tag{77}$$

This equation must be true whatever the differential changes dT and dP. Thus, it provides a relationship between h and l:

$$h = l\left(\frac{\partial V}{\partial P}\right)_T \tag{78}$$

and

$$l\left(\frac{\partial V}{\partial T}\right)_P = C_P - C_V \tag{79}$$

2.9.1.1. Expression of l. The differential entropy, dS, associated with this exchange is

$$dS = \frac{dQ}{T} = \frac{C_V}{T}dT + \frac{l}{T}dV = \left(\frac{\partial S}{\partial T}\right)_V dT + \left(\frac{\partial S}{\partial P}\right)_T dV \tag{80}$$

Writing that the second differentials $\partial^2 S/\partial T\partial V$ and $\partial^2 S/\partial V\partial T$ are equal, recognizing that $C_V/T = (\partial S/\partial T)_V$ and $l/T = (\partial S/\partial V)_T$, and deriving C_V/T by respect to V and l/T by respect to T gives

$$\left(\frac{\partial C_V}{\partial V}\right)_T = \left(\frac{\partial l}{\partial T}\right)_V - \frac{l}{T} \tag{81}$$

The differential energy, dU, is given by

$$dU = dQ + dW = dQ - P\,dV \tag{82}$$

where dW is the differential amount of work exchanged by the system. Combining Eqs. (80) and (82) gives

$$dU = C_V\,dT + (l - P)\,dV \tag{83}$$

Treating dU in the same way as dS above, through the equality of the second, cross partial differentials, leads to

$$\left(\frac{\partial C_V}{\partial V}\right)_T = \left(\frac{\partial l}{\partial T}\right)_V - \left(\frac{\partial P}{\partial T}\right)_V \tag{84}$$

The comparison of Eqs. (81) and (84) gives the value of l

$$l = T\left(\frac{\partial P}{\partial T}\right)_V \tag{85}$$

2.9.1.2. Expression of h. The differential entropy arising from the differential changes in T and P is given by

$$\mathrm{d}S = \frac{\mathrm{d}Q}{T} = \frac{C_P}{T}\,\mathrm{d}T + \frac{h}{T}\,\mathrm{d}P \tag{86}$$

Following a derivation similar to the one above, we write the differential enthalpy:

$$\begin{aligned}\mathrm{d}H = \mathrm{d}(U + PV) &= \mathrm{d}Q - P\,\mathrm{d}V + P\,\mathrm{d}V + V\,\mathrm{d}P \\ &= C_P\,\mathrm{d}T + (h + V)\,\mathrm{d}P\end{aligned} \tag{87}$$

Consideration of the equality of the second, cross partial differentials of S and H by respect to P and T leads to

$$h = -T\left(\frac{\partial V}{\partial T}\right)_P \tag{88}$$

2.9.2. Temperature increase occurring during carrier compression in the pump

As a first approximation, we consider that the compression of the mobile phase in the piston chamber of the pump occurs under reversible, adiabatic conditions. Then, there is no heat exchanged by the liquid with the surroundings and its entropy is kept constant. Then, letting dS be equal to 0 in Eq. (86) leads to

$$\left(\frac{\mathrm{d}T}{\mathrm{d}P}\right)_S = -\frac{h}{C_P} \tag{89}$$

which, combined with Eq. (88) gives

$$\left(\frac{\mathrm{d}T}{\mathrm{d}P}\right)_S = \frac{T}{C_P}\left(\frac{\partial V}{\partial T}\right)_P = \frac{\alpha T V}{C_P} \tag{90}$$

where α is the thermal expansion coefficient of the mobile phase defined as

$$\alpha = \frac{1}{V}\left(\frac{\partial V}{\partial T}\right)_P \tag{91}$$

All the quantities involved in Eq. (90) are positive. Thus, the compression of the mobile phase leads to an increase of its temperature. Eq. (90) is the basic equation for computing the temperature change of the mobile phase during its compression in the pump. To solve it, one needs an equation of state for this liquid, expressing the relationship between its volume, its temperature, and its pressure. Note that, in the above equations, because it was defined this way in Eq. (75a), C_P is an extensive property which depends on the mass of liquid considered. It is proportional to V, that is to the amount of liquid pumped.

Eq. (90) shows that the rate of variation of the temperature with the change in the pressure depends on parameters that are state quantities. Thus, $(\mathrm{d}T/\mathrm{d}P)_S$ is itself a state quantity, i.e., a thermodynamic property. It depends on the actual temperature and pressure.

Estimates of the value of $(\mathrm{d}T/\mathrm{d}P)_S$ for methanol at 25 °C, under 1 bar can be calculated, using data found in the literature [54]. For methanol, $C_P = 81.18\,\mathrm{J\,mol^{-1}\,K^{-1}}$, $\alpha = 1.204 \times 10^{-3}\,\mathrm{K^{-1}}$, $V = 1.2710\,\mathrm{cm^3\,g^{-1}}$ (i.e., $1.2710 \times 10^{-3}\,\mathrm{m^3\,kg^{-1}}$), $M_W = 32.04\,\mathrm{g\,mol^{-1}}$, giving $V = 4.072 \times 10^{-5}\,\mathrm{m^3\,mol^{-1}}$. These characteristics of methanol combine to give $(\mathrm{d}T/\mathrm{d}P)_S = 1.80 \times 10^{-7}\,\mathrm{K\,Pa^{-1}} = 1.80 \times 10^{-2}\,\mathrm{K\,bar^{-1}} = 18.0\,\mathrm{K/kbar}$. If this rate is independent of T and P, the temperature of methanol compressed to 1000 bar would be 18 K higher at the pump exit than at its initial temperature.

In fact, $(\mathrm{d}T/\mathrm{d}P)_S$ is not constant because V, C_P, and α depend on T and P. These dependencies can be calculated using an equation of state for the liquid. Such calculations have been performed and the results are available, tabulated as a function of T and P [54]. Using these data, $(\mathrm{d}T/\mathrm{d}P)_S$ has been calculated. Its variations with pressure are shown in Fig. 7 at different temperatures. It is seen that $(\mathrm{d}T/\mathrm{d}P)_S$ decreases with increasing pressure and increases with increasing temperature. When the pressure reaches 1000 bar and the temperature is around 40 °C, $(\mathrm{d}T/\mathrm{d}P)_S$ becomes equal to 11.5 K/kbar and the effect is only 2/3 of that calculated by assuming that the physico-chemical characteristics of methanol are constant.

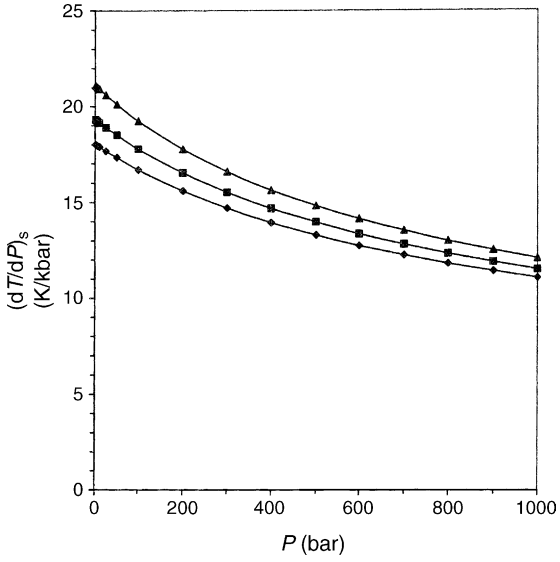

Fig. 7. Rate of increase of the temperature during the isoentropic compression of methanol, $(\mathrm{d}T/\mathrm{d}P)_S$ (K/kbar), vs. the final pressure for methanol, at different temperatures. From bottom to top, $T = 25$, 40, and 60 °C.

2.9.3. Temperature increase due to flow through a porous medium

In principle, the liquid flowing through the column would cool if it were decompressing under the same (quasi-adiabatic and reversible) conditions as those prevailing during its compression in the pump head and its temperature would be the same when it exits the column as its initial temperature, in the tank where the pump took it. Decompression is far slower than compression, however (in the ratio of the column to the stroke volumes). If the decompression takes place rapidly enough and the column walls are relatively thick, it can be considered again that no heat is exchanged with the surroundings of the column and that the decompression is adiabatic. It is then similar to the Joule–Thomson (Kelvin) process of expansion of a liquid though a porous plug. It is not entirely reversible, however, because the viscous dissipation must be taken into account. The latter takes place at constant enthalpy, H [53b]. For a perfect gas, this expansion takes place at constant temperature but for other fluids, a change in temperature arises from the change in pressure. It is a measure of the non-ideal behavior of the fluid.

Let $\mathrm{d}H$ be equal to 0 in Eq. (87), the temperature change resulting from the pressure change can be derived from Eq. (88) [53b,c]

$$\left(\frac{\mathrm{d}T}{\mathrm{d}P}\right)_H = -\frac{h+V}{C_P} = \frac{T(\partial V/\partial T)_P - V}{C_P} \tag{92}$$

Combining Eqs. (91) and (92) gives

$$-\left(\frac{\mathrm{d}T}{\mathrm{d}P}\right)_H = \frac{(1-\alpha T)V}{C_P} \tag{93}$$

For liquids under typical conditions (e.g., with T around 300 K), α is of the order of $1 \times 10^{-3}\,\mathrm{K}^{-1}$. Thus, Eq. (92) indicates that the temperature of the liquid increases with decreasing pressure when it percolates through a porous medium.

The quantity $-(\mathrm{d}T/\mathrm{d}P)_H$ appears to be also a thermodynamic quantity. Its variations with the temperature and the pressure are illustrated in Fig. 8. It increases with increasing pressure and decreases with increasing temperature. At 25 °C and under 1000 bar, the rate of temperature change is equal to 37.0 K/kbar while it it is only 26.5 K/kbar at 60 °C under 1 bar.

The comparison of Eqs. (90) and (93) shows that:

$$-\frac{(\mathrm{d}T/\mathrm{d}P)_H}{(\mathrm{d}T/\mathrm{d}P)_S} = \frac{1-\alpha T}{\alpha T} \tag{94}$$

Since αT is of the order of 1/3 at room temperature, it appears that the rate of increase of the temperature with a change in the pressure is about double during the decompression phase, when the mobile phase percolates through the column than during the compression phase, which takes place in the pump. This ratio depends, of course, on T and P.

It should be noted that if the chromatographic system (i.e., the pump, the connection lines, the injection device, and the column) is thermally well insulated, the two effects add together and the temperature of the carrier in the pump increases first during its compression in the pump and then, again, during its percolation through the column. If the column inlet pressure is sufficiently large, the outlet temperature may well exceed the boiling point of methanol under atmospheric pressure (65.0 °C). It might then be required to pressurize somewhat the column outlet in order to maintain the mobile phase in the liquid state.

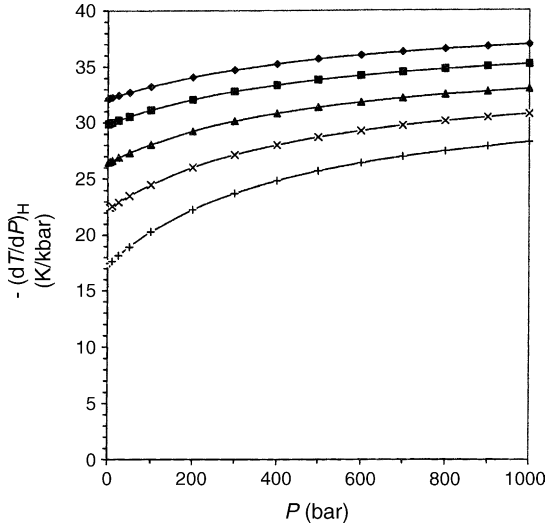

Fig. 8. Rate of increase of the temperature per unit decrease in the pressure, $-(\mathrm{d}T/\mathrm{d}P)_H$ (K/kbar), vs. the pressure during the isoenthalpic flow of methanol in an adiabatic column, at different temperatures. From bottom to top, T = 25, 40, 60, 80, and 100 °C.

2.9.4. Variation of the internal energy of the mobile phase during its compression in the pump

When the pressure increase by the amount $\mathrm{d}P$ in the piston chamber of the pump, the fluid temperature increases by $\mathrm{d}T$. Since the compression occurs adiabatically, there is no heat supplied by the pump to the carrier and the change, $\mathrm{d}U$, of the internal energy of the carrier results merely from the work of the pressure force, i.e., it is

$$\mathrm{d}U = -P\,\mathrm{d}V \tag{95}$$

Under adiabatic conditions, the changes of the temperature, the pressure, and the volume are related by $\mathrm{d}T = -(h/C_P)\,\mathrm{d}P$, according to Eq. (75a) and $\mathrm{d}T = -(l/C_V)\,\mathrm{d}V$, according to Eq. (75b). Thus, the volume and the pressure changes are related by

$$\mathrm{d}V = \frac{h}{l}\frac{C_V}{C_P}\,\mathrm{d}P \tag{96}$$

The value of h can be derived by combining Eqs. (88) and (91) as

$$h = -\alpha T V \tag{97}$$

Combining the definition of the mobile phase compressibility, χ (cf. Eq. (8)), with Eqs. (78) and (97), we can write

$$l = \frac{\alpha T}{\chi} \tag{98}$$

Combining Eqs. (79), (91), and (98) gives

$$C_P - C_V = \frac{\alpha^2 TV}{\chi} \tag{99}$$

Combining now Eqs. (97)–(99) gives the differential change in the internal energy during the compression of the mobile phase in the pump, as

$$\mathrm{d}U = \chi \frac{C_V}{C_P} VP\,\mathrm{d}P \tag{100a}$$

or

$$\mathrm{d}U = \chi \left(1 - \frac{\alpha^2 TV}{\chi C_P}\right) VP\,\mathrm{d}P \tag{100b}$$

If a state equation is available for the fluid involved, providing a relationship between P, V, T, α, χ, and C_P, Eq. (100b) can be integrated. This equation shows that the internal energy increases with increasing pressure (all the terms in Eq. (100a) are positive) and that this increase in the internal energy is caused by a finite compressibility ($\mathrm{d}U$ is equal to zero if $\chi = 0$).

If one assumes that all the quantities involved in Eq. (100b) are constant, independent of the pressure (except P, obviously), a first-order estimate of the energy stored is easily calculated. One obtains

$$\Delta U = \frac{\chi}{2} \frac{C_V}{C_P} V(P_\mathrm{i}^2 - P_0^2) = \frac{\chi}{2} \left(1 - \frac{\alpha^2 TV}{\chi C_P}\right) V(P_\mathrm{i}^2 - P_0^2) \tag{101}$$

As an example, for methanol we have $C_P = 82.29\,\mathrm{J\,mol^{-1}\,K^{-1}}$; $C_V = 69.65\,\mathrm{J\,mol^{-1}\,K^{-1}}$; $V = 1.2279\,\mathrm{cm^3\,g^{-1}}$; $\chi = 0.85 \times 10^{-4}\,\mathrm{bar^{-1}}$. For $P_\mathrm{i} = 1000\,\mathrm{bar}$ and $P_0 = 1\,\mathrm{bar}$, we obtain $\Delta U = 142\,\mathrm{Pa\,m^3\,mol^{-1}} = 4.42\,\mathrm{J\,g^{-1}}$. Although the rupture of the wall of a vessel under very high pressure can have devastating consequences, it is not an explosion and does not generate a shock wave. In HPLC, given the small amount of solvent compressed and the small amount of energy stored, it is unlikely that the loss consecutive to a rupture of the column will exceed much the cost of that column and of the work interrupted by the event.

2.9.5. Overall thermal effects

Contradictory claims are made in the recent literature. On the one hand, it is claimed that the influence of the thermal effect on the column efficiency becomes negligible when narrow bore columns are used. This has to result from the radial heat loss which reduces the radial temperature gradient in the column to a negligible value, thus avoiding the damaging consequences of a radial distribution of the mobile phase velocity across the column. In such a case, the consequences of the increase of the viscosity with increasing pressure will affect the dependence of the retention volume on the flow rate.

On the other hand, it is claimed that the heat effect, heating the mobile phase, hence reducing its viscosity, compensates the pressure dependence of the viscosity. This compensation can only be partial and limited. First, it is an overall compensation. At the beginning of the column, the viscosity remains higher than it is at room temperature and under atmospheric pressure, then it becomes lower at the end of the column, when the temperature of the mobile phase becomes high and the pressure low. Any change in the parameters that control such a balance will destroy it. For example, since the coefficients that characterize the pressure and temperature dependence of the viscosity are different for each solvent, a compensation can take place only for certain solvents, not for all. The extent of this compensation depends also on the radial heat loss, hence on the column inner diameter and thickness.

3. Results and discussion

A computer program can easily be written to implement the system of equations reported earlier. Calculations were made using the following set of parameters, a Young modulus E equal to $2 \times 10^6\,\mathrm{bar}$ (the value for stainless steel), a ratio $r_{\mathrm{ext},0}/r_{\mathrm{in},0}$ of the outer to the inner column radius equal to 2 (hence $a = 9.44 \times 10^{-7}\,\mathrm{bar^{-1}}$), a compressibility of the packing material β equal to $1 \times 10^6\,\mathrm{bar^{-1}}$, and an external column porosity ϵ_0 equal to 0.4. All the calculations made below neglect the influence of the thermal effect. Thus, the results are valid for narrow bore columns. For columns of more conventional size, the effects predicted are overestimated. Because the intensity of the heat effect and the corrections required are still rather unknown, it is not possible to go farther without making arbitrary assumptions. When more data will become available, this issue will have to be revisited.

3.1. Inlet pressure and flow rate

Fig. 9 illustrates the relationship between the actual pressure drop, $P_\mathrm{i} - P_0 = \Delta P$, that is required to achieve and maintain a certain constant outlet flow rate of methanol along an actual homogeneous column, and ΔP_id, the ideal pressure drop that would be needed, were all the pressure effects be negligible. Hence, in this ideal case, the mobile phase is supposed to be noncompressible, with a constant viscosity, independent of the local pressure, the packing material is also noncompressibe and the column tube is inelastic. The dashed line corresponds to the ideal case, $\Delta P = \Delta P_\mathrm{id}$. The three solid lines correspond to the cases in which only the pressure dependences of the viscosity, of the combined viscosity and density, and of the density of the mobile phase alone (from up to down, respectively) are taken into account. The thick black line corresponds to the results of calculations

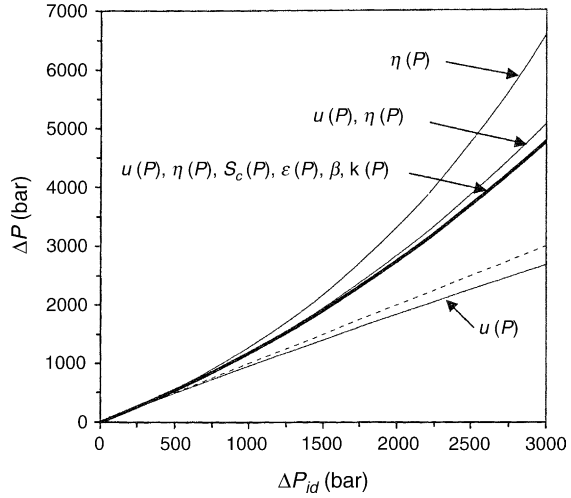

Fig. 9. Plot of the actual pressure drop, $\Delta P = P_i - P_0$, for methanol as a function of the pressure drop, ΔP_{id}, that would be obtained with the same flow rate of an ideal mobile phase, the density and viscosity of which are independent of the pressure, in an ideal column with incompressible packing and column metal (bold curve). The upper, lower, and medium curves correspond to cases in which only the effect of the pressure on the viscosity, the density, or both the viscosity and the density, respectively, is taken into account (light curves). The first diagonal (dashed line) is shown for reference.

performed when also taking into account the elasticity of the column wall and the compressibility of the packing material. Fig. 10 shows the relationship between $\Delta P/\Delta P_{id}$ versus ΔP_{id} and emphasizes the important deviations observed at high pressures, ca. 20% at 1000 bar and 60% at 3000 bar. Fig. 11 shows the relationship between $u_0/u_{0,id}$ and ΔP at constant inlet pressure.

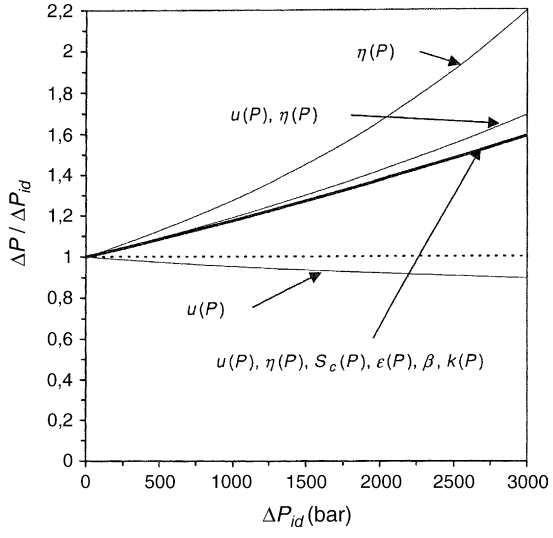

Fig. 10. Plot of the ratio of the actual pressure drop, ΔP, to the pressure drop, ΔP_{id}, that would be obtained for an ideal liquid in an ideal column versus ΔP_{id}, for methanol (bold curve). The upper, lower, and medium light curves correspond to the cases in which only the pressure-dependence of the viscosity, the density, or both the viscosity and the density, respectively, is taken into account.

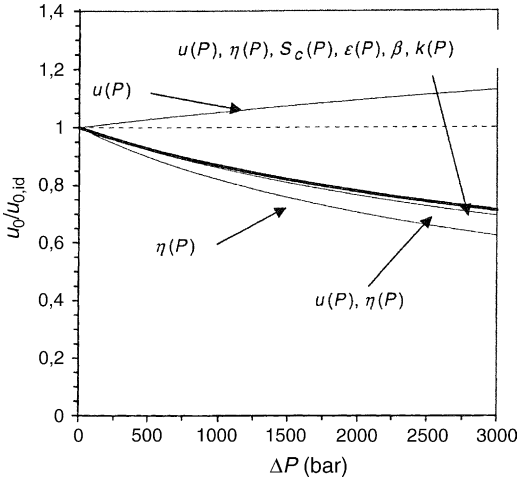

Fig. 11. Plot of the ratio of the actual outlet velocity of methanol, u_0, to the outlet velocity, $u_{0,id}$, that would be obtained, with the same inlet and outlet pressures, for an ideal liquid in an ideal column versus the inlet pressure, ΔP (bold curve). The lower, upper and medium light curves correspond to the cases in which only the pressure-dependence of the viscosity alone, the density alone, or of both the viscosity and the density, respectively, is taken into account.

These three figures show that the pressure dependence of the various properties characterizing the hydraulic behavior of HPLC columns combine to provide a markedly lower mobile phase flow rate through the column for a given pressure drop or a significantly higher pressure drop at a constant mass or outlet flow rate than could be predicted if these pressure effects were to be neglected. The effect is not linear and the inlet pressure must be increased proportionally more than the flow rate needs to be. It becomes quite important in the low kilobar range. The three figures show also that the elasticity of the column wall and the compressibility of the packing material contribute to reduce slightly the deviation of the flow rate dependence on the pressure from ideal behavior. For instance, if the flow rate velocity were such that the ideal pressure drop would be 2000 bar, the actual pressure drop is 2749 bar (i.e., 37.5% larger than in the ideal case), while it would be 2842 bar (i.e., 42.1% larger than in ideal case) for a column having an infinitely rigid wall and packed with an incompressible packing material. This result is due to the combination of the effects of the pressure-induced changes in the column permeability and in the column cross-sectional area available to the mobile phase.

3.2. Pressure and velocity profiles along the column

Fig. 12 compares the actual pressure profile of methanol along the column for three different inlet pressures, 1000, 2000, and 3000 bar, respectively (again, the dashed line corresponds to the ideal case). The deviations of the actual profiles from linear behavior are more clearly illustrated in Fig. 13 where the ratio of the local pressure gradient profile, $-\mathrm{d}P/\mathrm{d}z$, to the average pressure gradient, $\Delta P/L$ is plotted versus the

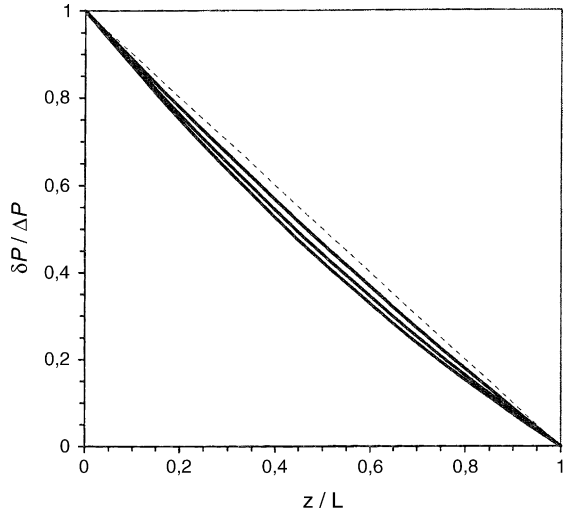

Fig. 12. Actual pressure profile along the column for methanol, expressed as the ratio of $\delta P = P - P_0$ to $\Delta P = P_i - P_0$ as a function of the ratio, z/L, of the abscissa, z, to column length, L. Actual pressure drop, ΔP, from upper to lower solid lines: 1000, 2000, and 3000 bar.

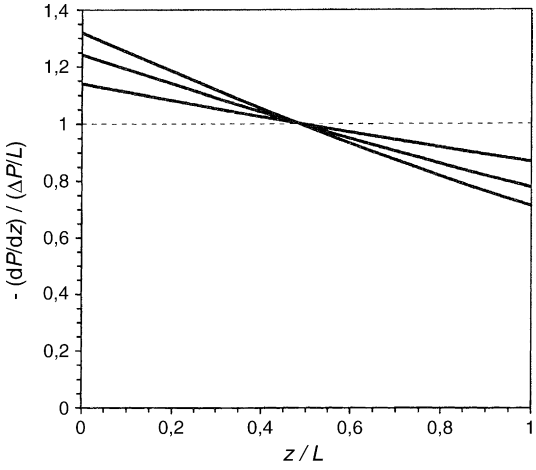

Fig. 13. Profile of the pressure gradient along the column for methanol, expressed as the ratio of the local absolute value of the actual gradient profile, $-\mathrm{d}P/\mathrm{d}z$, to the theoretical gradient, $\Delta P/L$, vs. z/L. Solvent: methanol. Three different values of the actual pressure drop, ΔP = 1000, 2000 and 3000 bar, from the lower to the upper full curves (near column inlet), respectively.

position in the column, for the same three cases, from lower (1000 bar) to upper (3000 bar) curves near the column inlet, respectively. These two sets of curves were calculated using Eqs. (62) to (64). Fig. 14 gives the velocity profile. Because the liquid is compressed under high pressures near the column inlet, its velocity is lower there than near the column outlet. The changes in the fluid velocity within the column are solely due to the pressure-dependence of the density, not to that of the viscosity. However, because the local velocity depends on the local pressure gradient and the pressure profile along the column is affected by the pressure-dependence of the viscosity, the velocity profile depends also on the velocity. It is seen that, for methanol, the inlet velocity is 8.9, 14.4 and 18.4% smaller than the outlet velocity when the pressure drop is 1000, 2000, and 3000 bar, respectively.

3.3. Pressure dependence of the hold-up time

The variation of $t_0/t_{0,id,1}$ (which is equal to $1/j$) versus ΔP_{id}, which is proportional to the value selected for u_0, and of $t_0/t_{0,id,2}$ versus ΔP are plotted for methanol in Figs. 15 and 16, respectively. The horizontal dashed lines of ordinate 1 in Figs. 15 and 16 show the situation in the ideal case. These figures show that, when one selects the flow rate (Fig. 15), the deviations from ideal behavior amount to 6.1, 11.9, and 17.6% for hypothetic pressure drops corresponding to the selected flow rate of 1000, 2000, and 3000 bar, respectively (the actual pressure drops are then 1176, 2749, and 4769 bar, respectively). If, instead, the column is operated under a selected inlet pressure (Fig. 16), the deviations of the hold-up time from ideal behavior are significantly larger and reach 21.3, 40.4, and 58.1%, when the actual pressure drops selected are 1000, 2000, and 3000 bar, respectively. In both cases, the deviations appear to increase almost linearly with the outlet velocity or with the selected pressure drop. Note that the situations treated earlier [47] correspond implicitly to the second case.

To illustrate the relative importance of the different contributions considered, the lower light full curve in Fig. 15 corresponds to the sole effect of the pressure dependence of the mobile phase density, i.e., to the case of a compressible mobile phase of constant viscosity equal to η_0. Note that, in the ideal case, $c = 0$, and $g(P) = h(P)$, so the deviation of t_0 from $t_{0,\mathrm{id},1}$ is solely due to compressibility of the mo-

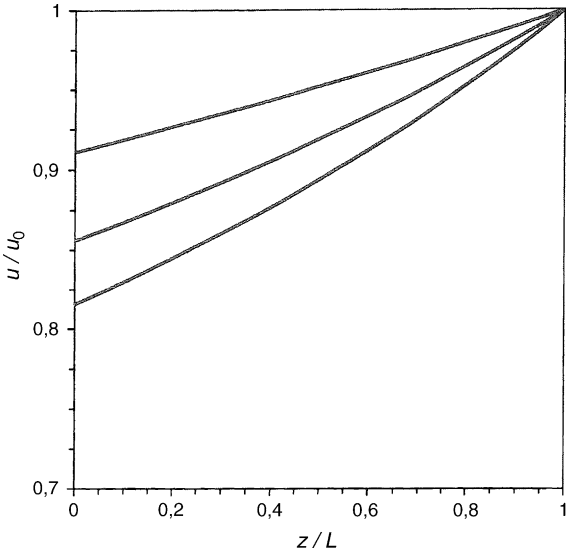

Fig. 14. Relative velocity profile, u/u_0, in the column, for methanol. From upper to lower curves: ΔP = 1000, 2000, and 3000 bar, respectively.

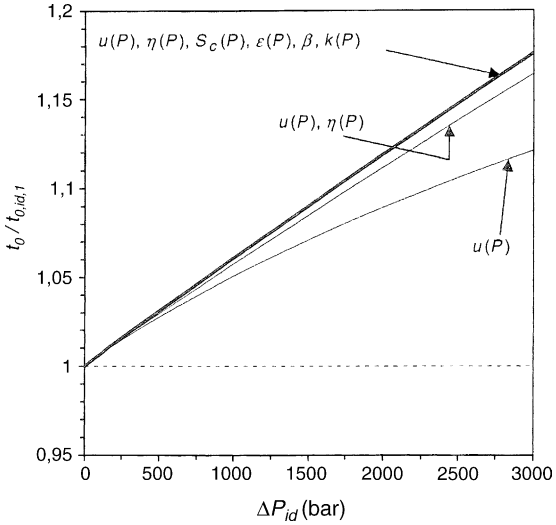

Fig. 15. Plot of the ratio of the actual hold-up time, t_0, to the theoretical hold-up time, $t_{0,\mathrm{id},1}$, observed with an ideal methanol, flowing at the same outlet velocity in an ideal column, versus the theoretical pressure drop, ΔP_{id}, required for these ideal liquid and column. The lower light full curve shows the influence of the sole effect of the pressure dependence of the density. The upper light curve shows the influence of the combined pressure dependences of the density and the viscosity of the mobile phase.

bile phase and the packing material and to the elasticity of the column tube, but not to the pressure dependence of the viscosity. However, the extent of this deviation depends on the actual inlet pressure. As this inlet pressure is larger for a compressible carrier of variable viscosity than for a similarly compressible carrier of constant viscosity, the deviation becomes larger for the former, actual carrier, as shown by the upper light solid curve. This curve differs little from the one obtained when the compressibility of the packing material and the elasticity of the tube are also taken into account (bold solid curve).

Similarly, the light full curves in Fig. 16 correspond to the sole effects of the pressure-dependences of the density and the viscosity of the mobile phase (methanol). However, the former is almost overlaid to the horizontal line of ordinate equal to 1 while the latter is almost overlaid to the bold curve corresponding to the influence of the pressure on the actual volumes occupied by the solvent, the packing material, and the column tube. This shows that, when the column is operated under constant inlet pressure, the deviation of the hold-up time from ideal behavior is almost entirely due to the pressure effect on the viscosity.

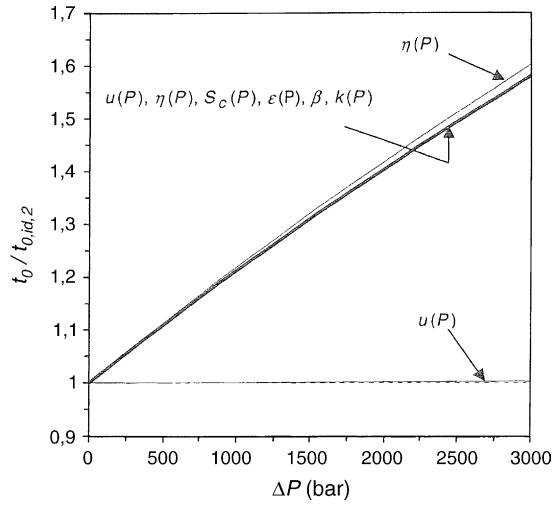

Fig. 16. Plot of the ratio of the actual hold-up time, t_0, to the theoretical hold-up time, $t_{0,\mathrm{id},2}$, observed with an ideal methanol, pumped into the column under the same pressure, versus the pressure drop, ΔP. The lower light full curve (almost completely overlaid with the dashed horizontal line of ordinate 1) illustrates the influence of the sole effect of the pressure dependence of the density. The upper light full curve (almost completely overlaid with the bold curve for the actual mobile phase and column) illustrates the sole effect of the pressure dependence of the viscosity.

3.4. Pressure and column dimensions

The variations of $S_c/S_{c,0}$ versus z/L are shown in Fig. 17 for three values of the pressure drop, 1000, 2000, and 3000 bar, from lower to upper curves, respectively. The initially cylindrical column at atmospheric pressure is elastically deformed under the influence of the pressure gradient and becomes approximately conical. Its internal geometrical volume consequently increases when the carrier is flowing. The area below a curve of Fig. 17 represents the fractional increase of the column geometrical volume resulting from carrier flow. It amounts to 0.090, 0.174, and 0.255% when the pressure drop along the column is, respectively, 1000, 2000, and 3000 bar.

Finally, Fig. 18 shows a plot of the permeability profile along the column. The pressure effect on k is relatively small, the permeability at the column inlet increasing by slightly less than 1.4%/kbar increase of the inlet pressure.

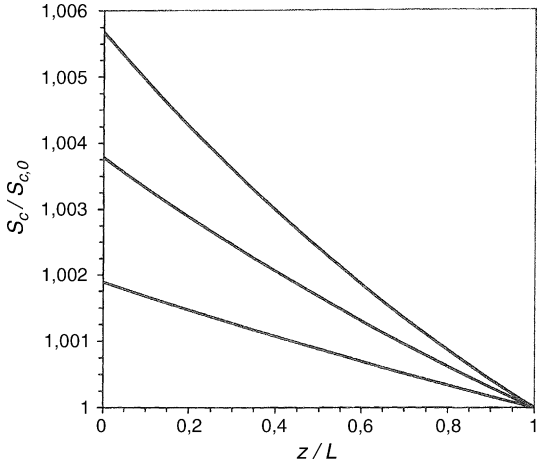

Fig. 17. Profile of the ratio of the column cross-sectional area, S_c to the cross-sectional area at column outlet, $S_{c,0}$, vs. z/L. Solvent: methanol. From lower to upper curves: $\Delta P = 1000$, 2000, and 3000 bar, respectively.

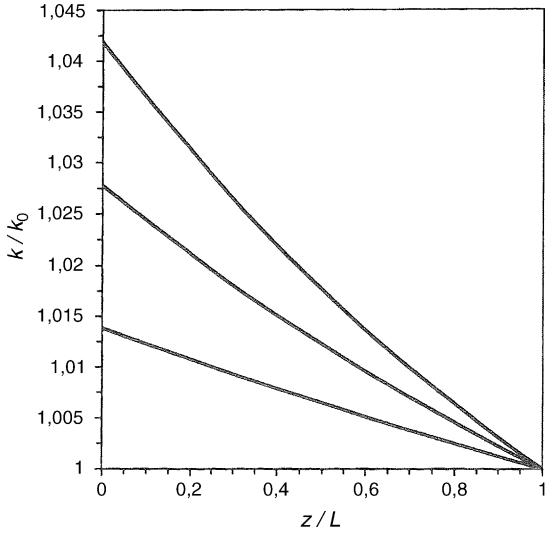

Fig. 18. Profile of the ratio of the column permeability, k to the permeability at column outlet, k_0, vs. z/L. Solvent: methanol. From lower to upper curves: $\Delta P = 1000$, 2000, and 3000 bar, respectively.

4. Conclusion

The primary goal of the analyst is the rapid and convenient achievement of accurate and reliable analytical results. From this point of view, the actual value of the inlet pressure set for a chromatographic separation is of minor importance. As long as the pumps operate within specifications, the reproducibility and the precision of the results should not be affected by the pressure set nor should the accuracy. However, serious difficulties will arise at the method development level. Any significant change in the flow rate will cause a change in the pressure profile along the column and all of the classical "constants" of a chromatographic separation, e.g., hold-up volume, column porosity, retention factors, efficiency coefficients, become variable. Optimization becomes too complex to be done easily following the time-honored method of trial-and-error. No computer programs are currently available that implement all the relationships discussed here. Even when they will be, the number of parameters that are required to carry out computer-assisted optimizations is very large. Those related to the solvents could be acquired relatively easily, although little is known at present regarding the quantitative behavior of solvent mixtures under very high pressures. Empirical rules could help to account for the influence of pressure on the equilibrium constants of analytes, hence on their separation factors. This might make the approach of computer assisted optimization difficult if even economically reasonable.

Acknowledgments

This work has been supported in part by Grant CHE-0244693 of the National Science Foundation and by the cooperative agreement between the University of Tennessee and the Oak Ridge National Laboratory. Fruitful discussions on pressure-induced column deformation with Jean-Claude Charmet and Pascal Kurowski (PMMH, ESPCI, Paris, France) and with F. Chen and E. Drumm (Department of Civil and Environmental Engineering, University of Tennessee, Knoxville, TN), on thermal effects with Jacques Leblond (PMMH, ESPCI, Paris, France) and on pressure-induced changes in liquid properties with Bernard Le Neindre (Laboratory of Material Engineering and High Pressures, University of Villetaneuse, France) are gratefully acknowledged.

References

[1] J.W. Jorgenson, Paper 1900–200, 2004 Pittsburgh Conference, 7–12 March 2004, Chicago, IL, USA.
[2] K. Nakanishi, N. Soga, J. Am. Ceram. Soc. 74 (1991) 2518.
[3] H. Minakuchi, K. Nakanishi, N. Soga, N. Ishizuka, N. Tanaka, Anal. Chem. 68 (1996) 3498.
[4] K. Miyabe, G. Guiochon, J. Sep. Sci. 27 (2004) 853.
[5] J.W. Jorgenson, E.J. Guthrie, J. Chromatogr. 255 (1983) 335.
[6] G. Guiochon, Anal. Chem. 53 (1981) 1318.
[7] R. Hayashi, Biochim. Biophys. Acta 1595 (2002) 397.
[8] S. Kunugi, N. Tanaka, Biochim. Biophys. Acta 1595 (2002) 329.
[9] M. Martin, G. Blu, C. Eon, G. Guiochon, J. Chromatogr. 112 (1975) 399.
[10] M. Martin, G. Blu, C. Eon, G. Guiochon, J. Chromatogr. 130 (1977) 458.
[11] M. Martin, G. Guiochon, J. Chromatogr. 151 (1978) 267.
[12] H. Colin, Personal communication, Palaiseau, 1980.
[13] W.J. Moore, Physical Chemistry, fourth ed., Prentice-Hall, Englewood Cliffs, 1972, pp. 211–213.
[14] F. Simon, G. Glatzel, Zeitschr. Anorg. Allgem. Chem. 178 (1929) 309.
[15] Techniques de l'Ingénieur, Paris, France, K 485, pp. 7–12.
[16] Anon, CRC Handbook of Chemistry and Physics, 60th ed., CRC Press, Boca Raton, FL, 1979–1980.
[17] Anon, Technical Data Book, The American Institute of Physics, 1964.
[18] P.W. Bridgman, The Physics of High Pressures, Dover, New York, NY, 1970.
[19] J.H. Dymond, R. Malhotra, Int. J. Thermophys. 9 (1988) 941.
[20] K. Lucas, Chem. Ing. Tech. 53 (1981) 959.
[21] B.E. Poling, J.M. Prausnitz, J.P. O'Connell, The Properties of Gases and Liquids, fifth ed., McGrawhill, New York, NY, 2001.
[22] J.S. Mellors, J.W. Jorgenson, Anal. Chem. 76 (2004) 5441.
[23] C.R. Wilke, P. Chang, AIChE J. 1 (1955) 264.
[24] M.T. Tyn, W.F. Calus, J. Chem. Eng. Data 20 (1975) 106.
[25] A.J. Easteal, AIChE J. 30 (1984) 641.
[26] S. Saeki, M. Tsubokawa, J. Yamanaka, T. Yamaguchi, Polymer 31 (1990) 2338.
[27] K.R. Harris, L.A. Woolf, J. Chem. Soc., Faraday Trans. I 76 (1980) 377.
[28] M. Martin, G. Guiochon, Anal. Chem. 55 (1983) 2302.
[29] T. Ikegami, E. Dicks, H. Kobayashi, H. Morisaka, D. Tokuda, K. Cabrera, K. Hosoya, N. Tanaka, J. Sep. Sci. 27 (2004) 1292.
[30] J.C. Giddings, P.D. Schettler, Anal. Chem. 36 (1964) 1483.
[31] G. Guiochon, A.M. Siouffi, J. Chromatogr. Sci. 16 (1978) 470.
[32] K.D. Patel, A.D. Jerkovich, J.C. Link, J.W. Jorgenson, Anal. Chem. 76 (2004) 5777.
[33] G. Guiochon, M.J. Sepaniak, J. Chromatogr. 606 (1992) 248.
[34] P. Szabelski, A. Cavazzini, K. Kaczmarski, X. Liu, G. Guiochon, J. Chromatogr. A 950 (2002) 41.
[35] H. Kim, F. Gritti, G. Guiochon, J. Chromatogr. A 1049 (2004) 25.

[36] X. Liu, D. Zhou, P. Szabelski, G. Guiochon, Anal. Chem. 75 (2003) 3999.
[37] S.-H. Chen, C.-T. Ho, K.-Y. Hsiao, J.-M. Chen, J. Chromatogr. A 891 (2000) 207.
[38] V.L. McGuffin, S.-H. Chen, Anal. Chem. 69 (1997) 930.
[39] N. Tanaka, T. Yoshimura, M. Araki, J. Chromatogr. 406 (1987) 247.
[40] B.A. Bidlingmeyer, R.P. Hooker, C.H. Lochmuller, L.B. Rogers, Sep. Sci. 4 (1969) 439.
[41] T.A. Maldacker, L.B. Rogers, Sep. Sci. 9 (1973) 27.
[42] G. Prukop, L.B. Rogers, Sep. Sci. 13 (1978) 59.
[43] F. Gritti, G. Guiochon, J. Chromatogr. A 1070 (2005) 1.
[44] S. Timoshenko, Résistance des Matériaux. 2ème Partie: Théorie Développée et Problèmes, 2ème édition, Librairie Polytechnique Ch. Béranger, Paris, 1954, pp. 213–217.
[45] H. Le Boiteux, La Mécanique des Solides Réels, Librairie Polytechnique Ch. Béranger, Paris, 1960, pp. 149–153.
[46] J. Mandel, Cours de Mécanique des milieux continus. Tome II. Mécanique des solides, Gauthier-Villars, Paris (France), 1966, pp. 503–505.
[47] M. Martin, G. Blu, G. Guiochon, J. Chromatogr. Sci. 11 (1973) 641.
[48] H.P.G. Darcy, Les Fontaines Publiques de la Ville de Dijon. Exposition et Application des Principes à Suivre et des Formules à Employer dans les Questions de Distribution d'Eau. Ouvrage Terminé par un Appendice Relatif aux Fournitures d'Eau de Plusieurs Villes, au Filtrage des Eaux et à la Fabrication des Tuyaux de Fonte, de Plomb, de Tôle et de Bitume, Victor Dalmont, Paris, France, 1856.
[49] A.T. James, A.J.P. Martin, Biochem. J. 50 (1952) 679–690.
[50] H. Poppe, J.C. Kraak, J.F.K. Huber, J.H.M. Van den Berg, Chromatographia 14 (1981) 515–523.
[51] H.-J. Lin, C. Horvath, Chem. Eng. Sci. 36 (1981) 47–55.
[52] H. Poppe, J.C. Kraak, Chromatogr. 282 (1983) 399–412.
[53] (a)Y. Rocard, Thermodynamique, second ed., Masson, Paris, 1967, p. 1;
(b)Y. Rocard, Thermodynamique, second ed., Masson, Paris, 1967, p. 8;
(c)Y. Rocard, Thermodynamique, second ed., Masson, Paris, 1967, p. 17 and 111.
[54] J.R.S. Machado, W.B. Street, J. Chem. Eng. Data 28 (1983) 218.